

Mitochondrial respiratory states and rates

COST Action CA15203 MitoEAGLE preprint Version: 2018-12-21 (51)

MitoEAGLE Task Group:

Gnaiger E, Aasander Frostner E, Abumrad NA, Acuna-Castroviejo D, Adiele RC, Ahn B, Ali SS, Alton L, Alves MG, Amati F, Amoedo ND, Andreadou I, Aragó M, Aral C, Arandarčikaitė O, Armand AS, Arnould T, Avram VF, Bailey DM, Bajpeyi S, Bajzikova M, Bakker BM, Barlow J, Bastos Sant'Anna Silva AC, Batterson P, Battino M, Bazil J, Beard DA, Bednarczyk P, Bello F, Ben-Shachar D, Bergdahl A, Berge RK, Bergmeister L, Bernardi P, Berridge MV, Bettinazzi S, Bishop D, Blier PU, Blindheim DF, Boardman NT, Boetker HE, Borchard S, Boros M, Børsheim E, Borutaite V, Botella J, Bouillaud F, Bouitbir J, Boushel RC, Bovard J, Breton S, Brown DA, Brown GC, Brown RA, Brozinick JT, Buettner GR, Burtscher J, Calabria E, Calbet JA, Calzia E, Cannon DT, Cano Sanchez M, Canto AC, Cardoso LHD, Carvalho E, Casado Pinna M, Cassar S, Cassina AM, Castelo MP, Castro L, Cavalcanti-de-Albuquerque JP, Cervinkova Z, Chabi B, Chakrabarti L, Chakrabarti S, Chaurasia B, Chen Q, Chicco AJ, Chinopoulos C, Chowdhury SK, Cizmarova B, Clementi E, Coen PM, Cohen BH, Coker RH, Collin A, Crisóstomo L, Dahdah N, Dalgaard LT, Dambrova M, Danhelovska T, Darveau CA, Das AM, Dash RK, Davidova E, Davis MS, De Goede P, De Palma C, Dembinska-Kiec A, Detraux D, Devaux Y, Di Marcello M, Dias TR, Distefano G, Doermann N, Doerrier C, Dong L, Donnelly C, Drahota Z, Duarte FV, Dubouchaud H, Duchon MR, Dumas JF, Durham WJ, Dymkowska D, Dyrstad SE, Dyson A, Dzialowski EM, Eaton S, Ehinger J, Elmer E, Endlicher R, Engin AB, Escames G, Ezrova Z, Falk MJ, Fell DA, Ferdinandy P, Ferko M, Ferreira JCB, Ferreira R, Ferri A, Fessel JP, Filipovska A, Fisar Z, Fischer C, Fischer M, Fisher G, Fisher JJ, Ford E, Fornaro M, Galina A, Galkin A, Gallee L, Galli GL, Gan Z, Ganetzky R, Garcia-Rivas G, Garcia-Roves PM, Garcia-Souza LF, Garipi E, Garlid KD, Garrabou G, Garten A, Gastaldelli A, Gayen J, Genders AJ, Genova ML, Giovarelli M, Goncalo Teixeira da Silva R, Goncalves DF, Gonzalez-Armenta JL, Gonzalez-Freire M, Gonzalo H, Goodpaster BH, Gorr TA, Gourlay CW, Granata C, Grefte S, Guarch ME, Gueguen N, Gumeni S, Haas CB, Haavik J, Haendeler J, Haider M, Hamann A, Han J, Han WH, Hancock CR, Hand SC, Handl J, Hargreaves IP, Harper ME, Harrison DK, Hausenloy DJ, Heales SJR, Heiestad C, Hellgren KT, Hepple RT, Hernansanz-Agustin P, Hewakapuge S, Hickey AJ, Ho DH, Hoehn KL, Hoel F, Holland OJ, Holloway GP, Hoppel CL, Hoppel F, Houstek J, Huete-Ortega M, Hyrossova P, Iglesias-Gonzalez J, Irving BA, Isola R, Iyer S, Jackson CB, Jadiya P, Jana PF, Jang DH, Jang YC, Janowska J, Jansen K, Jansen-Dürr P, Jansone B, Jarmuszkiewicz W, Jaskiewicz A, Jedlicka J, Jespersen NR, Jha RK, Jurczak MJ, Jurk D, Kaambre T, Kaczor JJ, Kainulainen H, Kampa RP, Kandel SM, Kane DA, Kapferer W, Kappler L, Karabatsiakos A, Karkucinska-Wieckowska A, Kaur S, Keijer J, Keller MA, Keppner G, Khamoui AV, Kidere D, Kilbaugh T, Kim HK, Kim JKS, Klepinin A, Klepinina L, Klingenspor M, Klocker H, Komlodi T, Koopman WJH, Kopitar-Jerala N, Kowaltowski AJ, Kozlov AV, Krajcova A, Krako Jakovljevic N, Kristal BS, Krycer JR, Kuang J, Kucera O, Kuka J, Kwak HB, Kwast K, Laasmaa M, Labieniec-Watala M, Lai N, Land JM, Lane N, Laner V, Lanza IR, Larsen TS, Lavery GG, Lazou A, Lee HK, Leeuwenburgh C, Lehti M, Lemieux H, Lenaz G, Lerfall J, Li PA, Li Puma L, Liepins E, Lionett S, Liu J, López LC, Lucchinetti E, Ma T, Macedo MP, Maciej S, MacMillan-Crow LA, Majtnerova P, Makarova E, Makrecka-Kuka M, Malik AN, Markova M, Martin DS, Martins AD, Martins JD, Maseko TE, Maull F, Mazat JP, McKenna HT, Menze MA, Merz T, Meszaros AT, Methner A, Michalak S, Moellering DR, Moiso N, Molina AJA, Montaigne D, Moore AL, Moreau K, Moreno-Sánchez R, Moreira BP, Mracek T, Muccini AM, Muntane J, Muntean DM, Murray AJ, Musiol E,

49 Myhre Pedersen T, Nair KS, Nehlin JO, Nemeč M, Neuffer PD, Neuzil J, Neviere R, Newsom S,
 50 Nozickova K, O'Brien KA, O'Gorman D, Olgar Y, Oliveira B, Oliveira MF, Oliveira MT, Oliveira PF,
 51 Oliveira PJ, Orynbayeva Z, Osiewacz HD, Pak YK, Pallotta ML, Palmeira CM, Parajuli N, Passos JF,
 52 Passrigger M, Patel HH, Pavlova N, Pecina P, Pereira da Silva Grilo da Silva F, Perez Valencia JA,
 53 Perks KL, Pesta D, Petit PX, Pettersen IKN, Pichaud N, Pichler I, Piel S, Pietka TA, Pino MF, Pirkmajer
 54 S, Plangger M, Porter C, Porter RK, Procaccio V, Prochownik EV, Prola A, Pulinilkunnil T, Puskarich
 55 MA, Puurand M, Radenkovic F, Ramzan R, Rattan SIS, Reboredo P, Renner-Sattler K, Rial E, Robinson
 56 MM, Roden M, Rodriguez E, Rodriguez-Enriquez S, Rohlena J, Rolo AP, Ropelle ER, Røsland GV,
 57 Rossignol R, Rossiter HB, Rubelj I, Rybacka-Mossakowska J, Saada A, Safaei Z, Saharnaz S, Salin K,
 58 Salvadego D, Sandi C, Saner N, Sanz A, Sazanov LA, Scatena R, Schartner M, Scheibye-Knudsen M,
 59 Schilling JM, Schlattner U, Schönfeld P, Schots PC, Schulz R, Schwarzer C, Scott GR, Selman C,
 60 Shabalina IG, Sharma P, Sharma V, Shevchuk I, Shirazi R, Siewiera K, Silber AM, Silva AM, Sims
 61 CA, Singer D, Singh BK, Skolik R, Smenes BT, Smith J, Soares FAA, Sobotka O, Sokolova I, Sonkar
 62 VK, Sowton AP, Sparagna GC, Sparks LM, Spinazzi M, Stankova P, Starr J, Stary C, Stelfa G, Stepto
 63 NK, Stiban J, Stier A, Stocker R, Storder J, Sumbalova Z, Suomalainen A, Suravajhala P, Svalbe B,
 64 Swerdlow RH, Swiniuch D, Szabo I, Szewczyk A, Szibor M, Tanaka M, Tandler B, Tarnopolsky MA,
 65 Tausan D, Tavernarakis N, Tepp K, Thakkar H, Thapa M, Thyfault JP, Tomar D, Ton R, Torp MK,
 66 Towheed A, Tretter L, Trewin AJ, Trifunovic A, Trivigno C, Tronstad KJ, Trougakos IP, Truu L,
 67 Tuncay E, Turan B, Tyrrell DJ, Urban T, Valentine JM, Van Bergen NJ, Van Hove J, Varricchio F,
 68 Vella J, Vendelin M, Vercesi AE, Victor VM, Vieira Ligo Teixeira C, Vidimce J, Viel C, Vieyra A,
 69 Vilks K, Villena JA, Vincent V, Vinogradov AD, Viscomi C, Vitorino RMP, Vogt S, Volani C, Volska
 70 K, Votion DM, Vujacic-Mirski K, Wagner BA, Ward ML, Warnsmann V, Wasserman DH, Watala C,
 71 Wei YH, Whitfield J, Wickert A, Wieckowski MR, Wiesner RJ, Williams CM, Winwood-Smith H,
 72 Wohlgemuth SE, Wohlwend M, Wolff JN, Wrutniak-Cabello C, Wüst RCI, Yokota T, Zablocki K,
 73 Zanon A, Zaugg K, Zaugg M, Zdrzilova L, Zhang Y, Zhang YZ, Ziková A, Zischka H, Zorzano A,
 74 Zvejniece L

75
76 Corresponding author: Gnaiger E

77 *Chair COST Action CA15203 MitoEAGLE* – <http://www.mitoeagle.org>

78 *Department of Visceral, Transplant and Thoracic Surgery, D. Swarovski Research Laboratory,*

79 *Medical University of Innsbruck, Innrain 66/4, A-6020 Innsbruck, Austria*

80 *Email: mitoeagle@i-med.ac.at; Tel: +43 512 566796, Fax: +43 512 566796 20*

81
82 522 coauthors

83
84 **Updates and discussion:**

85 http://www.mitoeagle.org/index.php/MitoEAGLE_preprint_States_and_rates



87	Table of contents
88	
89	Abstract
90	Executive summary
91	1. Introduction – Box 1: In brief: Mitochondria and Bioblasts
92	2. Coupling states and rates in mitochondrial preparations
93	2.1. <i>Cellular and mitochondrial respiration</i>
94	2.1.1. Aerobic and anaerobic catabolism and ATP turnover
95	2.1.2. Specification of biochemical dose
96	2.2. <i>Mitochondrial preparations</i>
97	2.3. <i>Electron transfer pathways</i>
98	2.4. <i>Respiratory coupling control</i>
99	2.4.1. Coupling
100	2.4.2. Phosphorylation, P _s , and P _s /O ₂ ratio
101	2.4.3. Uncoupling
102	2.5. <i>Coupling states and respiratory rates</i>
103	2.5.1. LEAK-state
104	2.5.2. OXPHOS-state
105	2.5.3. Electron transfer-state
106	2.5.4. ROX state and <i>Rox</i>
107	2.5.5. Quantitative relations
108	2.5.6. The steady-state
109	2.6. <i>Classical terminology for isolated mitochondria</i>
110	2.6.1. State 1
111	2.6.2. State 2
112	2.6.3. State 3
113	2.6.4. State 4
114	2.6.5. State 5
115	2.7. <i>Control and regulation</i>
116	3. What is a rate? – Box 2: Metabolic flows and fluxes: vectorial, vectorial, and scalar
117	4. Normalization of rate per sample
118	4.1. <i>Flow: per object</i>
119	4.1.1. Number concentration
120	4.1.2. Flow per object
121	4.2. <i>Size-specific flux: per sample size</i>
122	4.2.1. Sample concentration
123	4.2.2. Size-specific flux
124	4.3. <i>Marker-specific flux: per mitochondrial content</i>
125	4.3.1. Mitochondrial concentration and mitochondrial markers
126	4.3.2. mt-Marker-specific flux
127	5. Normalization of rate per system
128	5.1. <i>Flow: per chamber</i>
129	5.2. <i>Flux: per chamber volume</i>
130	5.2.1. System-specific flux
131	5.2.2. Advancement per volume
132	6. Conversion of units
133	7. Conclusions – Box 3: Recommendations for studies with mitochondrial preparations
134	Acknowledgements
135	Author contributions
136	Competing financial interests
137	References
138	Supplement
139	S1. Manuscript phases and versions - an open-access approach
140	S2. Joining COST Actions
141	

142 **Abstract** As the knowledge base and importance of mitochondrial physiology to human health expands,
 143 the necessity for harmonizing the terminology concerning mitochondrial respiratory states and rates has
 144 become increasingly apparent. The chemiosmotic theory establishes the mechanism of energy
 145 transformation and coupling in oxidative phosphorylation. The unifying concept of the protonmotive
 146 force provides the framework for developing a consistent theoretical foundation of mitochondrial
 147 physiology and bioenergetics. We follow guidelines of the International Union of Pure and Applied
 148 Chemistry (IUPAC) on terminology in physical chemistry, extended by considerations of open systems
 149 and thermodynamics of irreversible processes. The concept-driven constructive terminology
 150 incorporates the meaning of each quantity and aligns concepts and symbols with the nomenclature of
 151 classical bioenergetics. We endeavour to provide a balanced view of mitochondrial respiratory control
 152 and a critical discussion on reporting data of mitochondrial respiration in terms of metabolic flows and
 153 fluxes. Uniform standards for evaluation of respiratory states and rates will ultimately contribute to
 154 reproducibility between laboratories and thus support the development of databases of mitochondrial
 155 respiratory function in species, tissues, and cells. Clarity of concept and consistency of nomenclature
 156 facilitate effective transdisciplinary communication, education, and ultimately further discovery.

157
 158 *Keywords:* Mitochondrial respiratory control, coupling control, mitochondrial preparations,
 159 protonmotive force, uncoupling, oxidative phosphorylation: OXPHOS, efficiency, electron transfer: ET,
 160 electron transfer system: ETS, proton leak, ion leak and slip compensatory state: LEAK, residual oxygen
 161 consumption: ROX, State 2, State 3, State 4, normalization, flow, flux, oxygen: O₂
 162

163 **Executive summary**

164
 165 In view of the broad implications for health care, mitochondrial researchers face an increasing
 166 responsibility to disseminate their fundamental knowledge and novel discoveries to a wide range of
 167 stakeholders and scientists beyond the group of specialists. This requires implementation of a commonly
 168 accepted terminology within the discipline and standardization in the translational context. Authors,
 169 reviewers, journal editors, and lecturers are challenged to collaborate with the aim to harmonize the
 170 nomenclature in the growing field of mitochondrial physiology and bioenergetics, from evolutionary
 171 biology and comparative physiology to mitochondrial medicine. In the present communication we focus
 172 on the following concepts in mitochondrial physiology:

- 173 1. Aerobic respiration depends on the coupling of phosphorylation (ADP → ATP) to O₂ flux in
 174 catabolic reactions. Coupling in oxidative phosphorylation is mediated by the translocation of
 175 protons across the mitochondrial inner membrane (mtIM) through proton pumps generating
 176 or utilizing the protonmotive force that is maintained between the mitochondrial matrix and
 177 intermembrane compartment or outer mitochondrial space. Compartmental coupling depends
 178 on ion translocation across a semipermeable membrane, which is defined as vectorial
 179 metabolism and distinguishes oxidative phosphorylation from cytosolic fermentation as
 180 counterparts of cellular core energy metabolism (**Figure 1**). Cell respiration is thus
 181 distinguished from fermentation: (1) Electron acceptors are supplied by external respiration
 182 for the maintenance of redox balance, whereas fermentation is characterized by an internal
 183 electron acceptor produced in intermediary metabolism. In aerobic cell respiration, redox
 184 balance is maintained by O₂ as the electron acceptor. (2) Compartmental coupling in vectorial
 185 oxidative phosphorylation contrasts to exclusively scalar substrate-level phosphorylation in
 186 fermentation.
- 187 2. When measuring mitochondrial metabolism, the contribution of fermentation and other cytosolic
 188 interactions must be excluded from analysis by disrupting the barrier function of the plasma
 189 membrane. Selective removal or permeabilization of the plasma membrane yields
 190 mitochondrial preparations—including isolated mitochondria, tissue and cellular
 191 preparations—with structural and functional integrity. Subsequently, extra-mitochondrial
 192 concentrations of fuel substrates, ADP, ATP, inorganic phosphate, and cations including H⁺
 193 can be controlled to determine mitochondrial function under a set of conditions defined as
 194 coupling control states. We strive to incorporate an easily recognized and understood concept-
 195 driven terminology of bioenergetics with explicit terms and symbols that define the nature of
 196 respiratory states.

- 197 3. Mitochondrial coupling states are defined according to the control of respiratory oxygen flux by
 198 the protonmotive force. Capacities of oxidative phosphorylation and electron transfer are
 199 measured at kinetically saturating concentrations of fuel substrates, ADP and inorganic
 200 phosphate, and O₂, or at optimal uncoupler concentrations, respectively, in the absence of
 201 Complex IV inhibitors such as NO, CO, or H₂S. Respiratory capacity is a measure of the upper
 202 boundary of the rate of respiration; it depends on the substrate type undergoing oxidation, and
 203 provides reference values for the diagnosis of health and disease, and for evaluation of the
 204 effects of Evolutionary background, Age, Gender and sex, Lifestyle and Environment.
 205

206 Figure 1. Internal and external respiration

207 Mitochondrial respiration is the oxidation of fuel
 208 substrates (electron donors) and reduction of O₂
 209 catalysed by the electron transfer system, ETS:
 210 (mt) mitochondrial catabolic respiration; (ce)
 211 total cellular O₂ consumption; and (ext) external
 212 respiration. All chemical reactions, *r*, that
 213 consume O₂ in the cells of an organism,
 214 contribute to cell respiration, *J*_{O₂}. In addition to
 215 mitochondrial catabolic respiration, O₂ is
 216 consumed by:

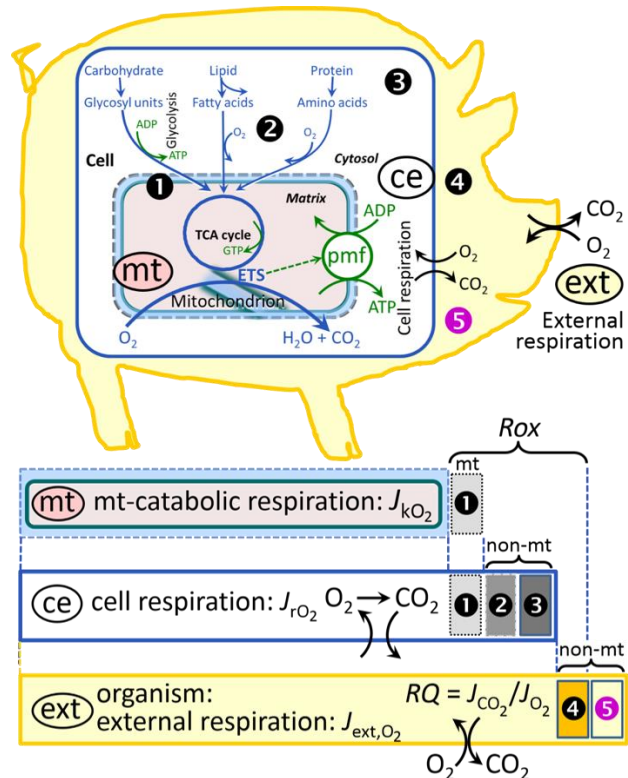
217 ❶ Mitochondrial residual oxygen consumption,
 218 *Rox*. ❷ Non-mitochondrial O₂ consumption by
 219 catabolic reactions, particularly peroxisomal
 220 oxidases and microsomal cytochrome P450
 221 systems. ❸ Non-mitochondrial *Rox* by reactions
 222 unrelated to catabolism. ❹ Extracellular *Rox*. ❺
 223 Aerobic microbial respiration. Bars are not at a
 224 quantitative scale.

225 (mt) **Mitochondrial catabolic respiration**, *J*_{KO₂},
 226 is the O₂ consumption by the mitochondrial
 227 ETS excluding *Rox*.

228 (ce) **Cell respiration**, *J*_{rO₂}, takes into account
 229 internal O₂-consuming reactions, *r*, including catabolic respiration and *Rox*. Catabolic cell respiration
 230 is the O₂ consumption associated with catabolic pathways in the cell, including mitochondrial
 231 catabolism in addition to peroxisomal and microsomal oxidation reactions (❷).

232 (ext) **External respiration** balances internal respiration at steady-state, including extracellular *Rox* (❹)
 233 and aerobic respiration by the microbiome (❺). O₂ is transported from the environment across the
 234 respiratory cascade, *i.e.*, circulation between tissues and diffusion across cell membranes, to the
 235 intracellular compartment. The respiratory quotient, *RQ*, is the molar CO₂/O₂ exchange ratio; when
 236 combined with the respiratory nitrogen quotient, N/O₂ (mol N given off per mol O₂ consumed), the
 237 *RQ* reflects the proportion of carbohydrate, lipid and protein utilized in cell respiration during
 238 aerobically balanced steady-states. Bicarbonate and CO₂ are transported in reverse to the
 239 extracellular milieu and the organismic environment. Hemoglobin provides the molecular paradigm
 240 for the combination of O₂ and CO₂ exchange, as do lungs and gills on the morphological level.
 241 Consult **Table 8** for a list of terms and symbols.
 242

- 243 4. Incomplete tightness of coupling, *i.e.*, some degree of uncoupling relative to the substrate-
 244 dependent coupling stoichiometry, is a characteristic of energy-transformations across
 245 membranes. Uncoupling is caused by a variety of physiological, pathological, toxicological,
 246 pharmacological and environmental conditions that exert an influence not only on the proton
 247 leak and cation cycling, but also on proton slip within the proton pumps and the structural
 248 integrity of the mitochondria. A more loosely coupled state is induced by stimulation of
 249 mitochondrial superoxide formation and the bypass of proton pumps. In addition, the use of
 250 protonophores represents an experimental uncoupling intervention to assess the transition
 251 from a well-coupled to a noncoupled state of mitochondrial respiration.



- 252 5. Respiratory oxygen consumption rates have to be carefully normalized to enable meta-analytic
 253 studies beyond the question of a particular experiment. Therefore, all raw data on rates and
 254 variables for normalization should be published in an open access data repository.
 255 Normalization of rates for: (1) the number of objects (cells, organisms); (2) the volume or
 256 mass of the experimental sample; and (3) the concentration of mitochondrial markers in the
 257 experimental chamber are sample-specific normalizations, which are distinguished from
 258 system-specific normalization for the volume of the chamber (the measuring system).
- 259 6. The consistent use of terms and symbols will facilitate transdisciplinary communication and
 260 support the further development of a collaborative database on bioenergetics and
 261 mitochondrial physiology. The present considerations are focused on studies with
 262 mitochondrial preparations. These will be extended in a series of reports on pathway control
 263 of mitochondrial respiration, respiratory states in intact cells, and harmonization of
 264 experimental procedures.
 265

266 **Box 1: In brief – Mitochondria and Bioblasts**

267 *‘For the physiologist, mitochondria afforded the first opportunity for an experimental*
 268 *approach to structure-function relationships, in particular those involved in active*
 269 *transport, vectorial metabolism, and metabolic control mechanisms on a subcellular level’*
 270 *(Ernster and Schatz 1981).*

271 Mitochondria are oxygen-consuming electrochemical generators that evolved from the endosymbiotic
 272 alphaproteobacteria which became integrated into a host cell related to Asgard Archaea (Margulis 1970;
 273 Lane 2005; Roger *et al.* 2017). They were described by Richard Altmann (1894) as ‘bioblasts’, which
 274 include not only the mitochondria as presently defined, but also symbiotic and free-living bacteria. The
 275 word ‘mitochondria’ (Greek mitos: thread; chondros: granule) was introduced by Carl Benda (1898).
 276 Mitochondrion is singular and mitochondria is plural. Abbreviation: mt, as generally used in mtDNA.

277 Contrary to current textbook dogma, which describes mitochondria as individual organelles,
 278 mitochondria form dynamic networks within eukaryotic cells. Mitochondrial movement is supported by
 279 microtubules and morphology can change in response to energy requirements of the cell via processes
 280 known as fusion and fission; these interactions allow mitochondria to communicate within a network
 281 (Chan 2006). Mitochondria can even traverse cell boundaries in a process known as horizontal
 282 mitochondrial transfer (Torralba *et al.* 2016). Another defining characteristic of mitochondria is the
 283 double membrane. The mitochondrial inner membrane (mtIM) forms dynamic tubular to disk-shaped
 284 cristae that separate the mitochondrial matrix, *i.e.*, the negatively charged internal mitochondrial
 285 compartment, from the intermembrane space; the latter being enclosed by the mitochondrial outer
 286 membrane (mtOM) and positively charged with respect to the matrix.

287 The mtIM contains the non-bilayer phospholipid cardiolipin, which is not present in any other
 288 eukaryotic cellular membrane. Cardiolipin has many regulatory functions (Oemer *et al.* 2018); in
 289 particular, it stabilizes and promotes the formation of respiratory supercomplexes (SC I_nIII_nIV_n), which
 290 are supramolecular assemblies based upon specific and dynamic interactions between individual
 291 respiratory complexes (Greggio *et al.* 2017; Lenaz *et al.* 2017). The mitochondrial membrane is plastic
 292 and exerts an influence on the functional properties of proteins incorporated in membranes
 293 (Waczulikova *et al.* 2007). Intracellular stress factors may cause shrinking or swelling of the
 294 mitochondrial matrix that can ultimately result in permeability transition (mtPT; Lemasters *et al.* 1998).

295 Mitochondria constitute the structural and functional elementary components of cell respiration.
 296 Mitochondrial respiration is the reduction of molecular oxygen by electron transfer coupled to
 297 electrochemical proton translocation across the mtIM. In the process of oxidative phosphorylation
 298 (OXPHOS), the catabolic reaction of oxygen consumption is electrochemically coupled to the
 299 transformation of energy in the form of adenosine triphosphate (ATP; Mitchell 1961, 2011).
 300 Mitochondria are the powerhouses of the cell that contain the machinery of the OXPHOS-pathways,
 301 including transmembrane respiratory complexes (proton pumps with FMN, Fe-S and cytochrome *b*, *c*,
 302 *aa*₃ redox systems); alternative dehydrogenases and oxidases; the coenzyme ubiquinone (Q); F-ATPase
 303 or ATP synthase; the enzymes of the tricarboxylic acid cycle (TCA), fatty acid and amino acid oxidation;
 304 transporters of ions, metabolites and co-factors; iron/sulphur cluster synthesis; and mitochondrial
 305 kinases related to catabolic pathways. The mitochondrial proteome comprises over 1,200 proteins
 306 (Calvo *et al.* 2015; 2017), mostly encoded by nuclear DNA (nDNA), with a variety of functions, many
 307 of which are relatively well known, *e.g.*, proteins regulating mitochondrial biogenesis or apoptosis,

308 while others are still under investigation, or need to be identified, *e.g.*, mtPT pore, alanine transporter.
 309 The mammalian mitochondrial proteome can be used to discover and characterize the genetic basis of
 310 mitochondrial diseases (Williams *et al.* 2016; Palmfeldt and Bross 2017).

311 Numerous cellular processes are orchestrated by a constant crosstalk between mitochondria and
 312 other cellular components. For example, the crosstalk between mitochondria and the endoplasmic
 313 reticulum is involved in the regulation of calcium homeostasis, cell division, autophagy, differentiation,
 314 and anti-viral signaling (Murley and Nunnari 2016). Mitochondria contribute to the formation of
 315 peroxisomes, which are hybrids of mitochondrial and ER-derived precursors (Sugiura *et al.* 2017).
 316 Cellular mitochondrial homeostasis (mitostasis) is maintained through regulation at transcriptional,
 317 post-translational and epigenetic levels, resulting in dynamic regulation of mitochondrial turnover by
 318 biogenesis of new mitochondria and removal of damaged mitochondria by fusion, fission and mitophagy
 319 (Singh *et al.* 2018). Cell signalling modules contribute to homeostatic regulation throughout the cell
 320 cycle or even cell death by activating proteostatic modules, *e.g.*, the ubiquitin-proteasome and
 321 autophagy-lysosome/vacuole pathways; specific proteases like LON, and genome stability modules in
 322 response to varying energy demands and stress cues (Quiros *et al.* 2016). Several post-translational
 323 modifications, including acetylation and nitrosylation, are also capable of influencing the bioenergetic
 324 response, with clinically significant implications for health and disease (Carrico *et al.* 2018).

325 Mitochondria of higher eukaryotes typically maintain several copies of their own circular genome
 326 known as mitochondrial DNA (mtDNA; hundred to thousands per cell; Cummins 1998), which is
 327 maternally inherited in many species. However, biparental mitochondrial inheritance is documented in
 328 some exceptional cases in humans (Luo *et al.* 2018), is widespread in birds, fish, reptiles and invertebrate
 329 groups, and is even the norm in some bivalve taxonomic groups (Breton *et al.* 2007; White *et al.* 2008).
 330 The mitochondrial genome of the angiosperm *Amborella* contains a record of six mitochondrial genome
 331 equivalents acquired by horizontal transfer of entire genomes, two from angiosperms, three from algae
 332 and one from mosses (Rice *et al.* 2016). In unicellular organisms, *i.e.*, protists, the structural organization
 333 of mitochondrial genomes is highly variable and includes circular and linear DNA (Zikova *et al.* 2016).
 334 While some of the free-living flagellates exhibit the largest known gene coding capacity, *e.g.*, jakobid
 335 *Andalucia godoyi* mitochondrial DNA codes for 106 genes (Burger *et al.* 2013), some protist groups,
 336 *e.g.*, alveolates, possess mitochondrial genomes with only three protein-coding genes and two rRNAs
 337 (Feagin *et al.* 2012). The complete loss of mitochondrial genome is observed in the highly reduced
 338 mitochondria of *Cryptosporidium* species (Liu *et al.* 2016). Reaching the final extreme, the microbial
 339 eukaryote, oxymonad *Monocercomonoides*, has no mitochondrion whatsoever and lacks all typical
 340 nuclear-encoded mitochondrial proteins, showing that while in 99% of organisms mitochondria play a
 341 vital role, this organelle is not indispensable (Karnkowska *et al.* 2016).

342 In vertebrates, but not all invertebrates, mtDNA is compact (16.5 kB in humans) and encodes 13
 343 protein subunits of the transmembrane respiratory Complexes CI, CIII, CIV and ATP synthase (F-
 344 ATPase), 22 tRNAs, and two ribosomal RNAs. Additional gene content has been suggested to include
 345 microRNAs, piRNA, smithRNAs, repeat associated RNA, long noncoding RNAs, and even additional
 346 proteins or peptides (Rackham *et al.* 2011; Duarte *et al.* 2014; Lee *et al.* 2015; Cobb *et al.* 2016). The
 347 mitochondrial genome requires nuclear-encoded mitochondrially targeted proteins, *e.g.*, TFAM, for its
 348 maintenance and expression (Rackham *et al.* 2012). The nuclear and the mitochondrial genomes encode
 349 peptides of the membrane spanning redox pumps (CI, CIII and CIV) and F-ATPase, leading to strong
 350 constraints in the coevolution of both genomes (Blier *et al.* 2001).

351 Given the multiple roles of mitochondria, it is perhaps not surprising that mitochondrial
 352 dysfunction is associated with a wide variety of genetic and degenerative diseases. Robust mitochondrial
 353 function is supported by physical exercise and caloric balance, and is central for sustained metabolic
 354 health throughout life. Therefore, a more consistent set of definitions for mitochondrial physiology will
 355 increase our understanding of the etiology of disease and improve the diagnostic repertoire of
 356 mitochondrial medicine with a focus on protective medicine, lifestyle and healthy aging.
 357

358
 359

360 1. Introduction

361
 362
 363

Mitochondria are the powerhouses of the cell with numerous physiological, molecular, and genetic functions (**Box 1**). Every study of mitochondrial health and disease faces **Evolution, Age,**

364 **Gender and sex, Lifestyle, and Environment (MitoEAGLE)** as essential background conditions intrinsic
 365 to the individual person or cohort, species, tissue and to some extent even cell line. As a large and
 366 coordinated group of laboratories and researchers, the mission of the global MitoEAGLE Network is to
 367 generate the necessary scale, type, and quality of consistent data sets and conditions to address this
 368 intrinsic complexity. Harmonization of experimental protocols and implementation of a quality control
 369 and data management system are required to interrelate results gathered across a spectrum of studies
 370 and to generate a rigorously monitored database focused on mitochondrial respiratory function. In this
 371 way, researchers from a variety of disciplines can compare their findings using clearly defined and
 372 accepted international standards.

373 With an emphasis on quality of research, published data can be useful far beyond the specific
 374 question of a particular experiment. For example, collaborative data sets support the development of
 375 open-access databases such as those for National Institutes of Health sponsored research in genetics,
 376 proteomics, and metabolomics. Indeed, enabling meta-analysis is the most economic way of providing
 377 robust answers to biological questions (Cooper *et al.* 2009). However, the reproducibility of quantitative
 378 results and databases depend on accurate measurements under strictly-defined conditions. Likewise,
 379 meaningful interpretation and comparability of experimental outcomes requires standardisation of
 380 protocols between research groups at different institutes. In addition to quality control, a conceptual
 381 framework is also required to standardise and harmonise terminology and methodology. Vague or
 382 ambiguous jargon can lead to confusion and may convert valuable signals to wasteful noise. For this
 383 reason, measured values must be expressed in standard units for each parameter used to define
 384 mitochondrial respiratory function. A consensus on fundamental nomenclature and conceptual
 385 coherence, however, are missing in the expanding field of mitochondrial physiology. To fill this gap,
 386 the present communication provides an in-depth review on harmonization of nomenclature and
 387 definition of technical terms, which are essential to improve the awareness of the intricate meaning of
 388 current and past scientific vocabulary. This is important for documentation and integration into
 389 databases in general, and quantitative modelling in particular (Beard 2005).

390 In this review, we focus on coupling states and fluxes through metabolic pathways of aerobic
 391 energy transformation in mitochondrial preparations as a first step in the attempt to generate a
 392 conceptually-oriented nomenclature in bioenergetics and mitochondrial physiology. Respiratory control
 393 by fuel substrates and specific inhibitors of respiratory enzymes, coupling states of intact cells, and
 394 respiratory flux control ratios will be reviewed in subsequent communications, prepared in the frame of
 395 the EU COST Action MitoEAGLE open to global bottom-up input.

396
397

398 **2. Coupling states and rates in mitochondrial preparations**

399 *‘Every professional group develops its own technical jargon for talking about matters of critical*
 400 *concern ... People who know a word can share that idea with other members of their group, and*
 401 *a shared vocabulary is part of the glue that holds people together and allows them to create a*
 402 *shared culture’* (Miller 1991).

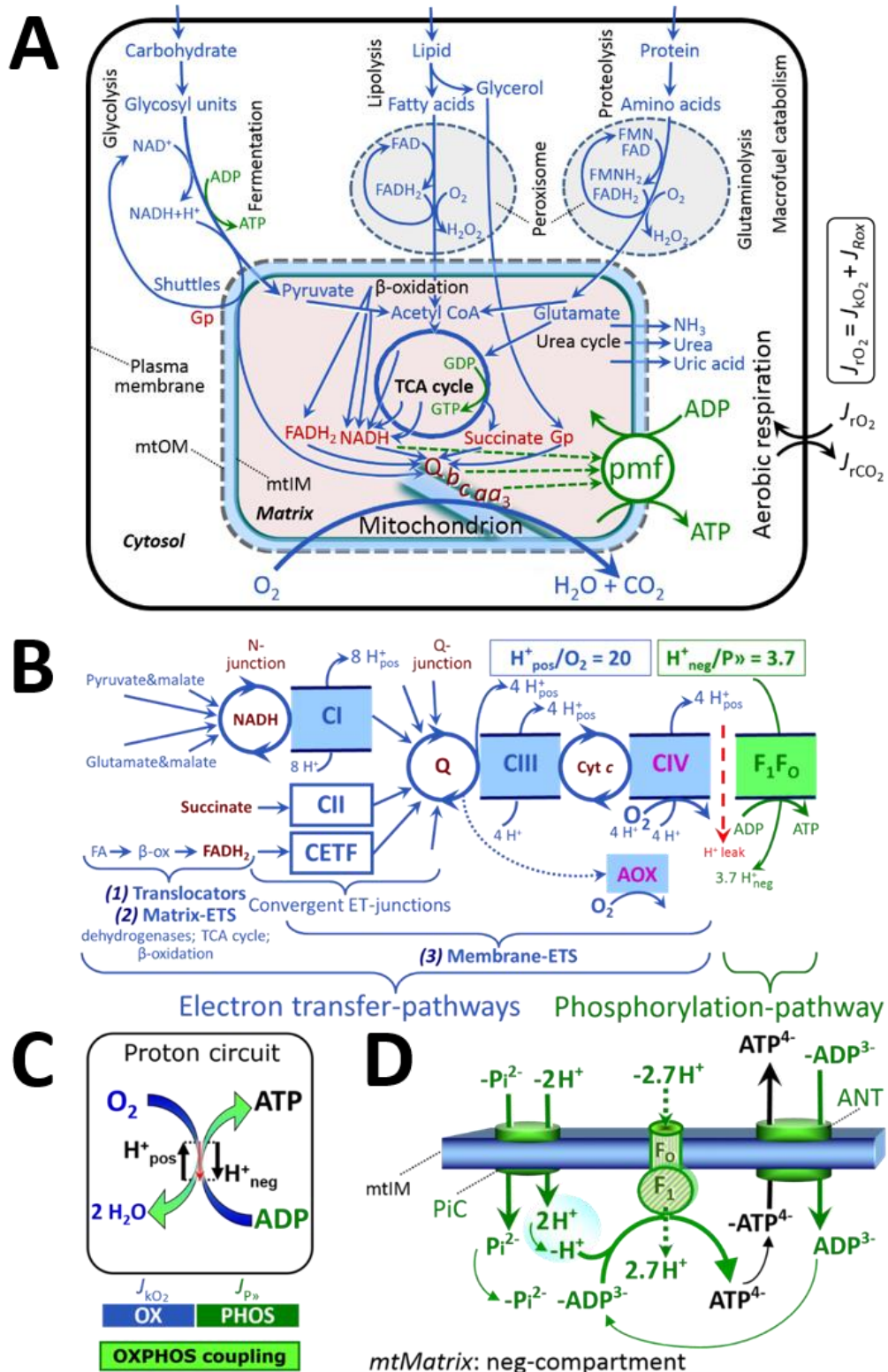
403

404 *2.1. Cellular and mitochondrial respiration*

405

406 **2.1.1. Aerobic and anaerobic catabolism and ATP turnover:** In respiration, electron transfer
 407 is coupled to the phosphorylation of ADP to ATP, with energy transformation mediated by the
 408 protonmotive force, pmf (**Figure 2**). Anabolic reactions are coupled to catabolism, both by ATP as the
 409 intermediary energy currency and by small organic precursor molecules as building blocks for
 410 biosynthesis. Glycolysis involves substrate-level phosphorylation of ADP to ATP in fermentation
 411 without utilization of O₂, studied mainly in intact cells and organisms. Many cellular fuel substrates are
 412 catabolized to acetyl-CoA or to glutamate, and further electron transfer reduces nicotinamide adenine
 413 dinucleotide to NADH or flavin adenine dinucleotide to FADH₂. Subsequent mitochondrial electron
 414 transfer to O₂ is coupled to proton translocation for the control of the protonmotive force and
 415 phosphorylation of ADP (**Figure 2B and 2C**). In contrast, extra-mitochondrial oxidation of fatty acids
 416 and amino acids proceeds partially in peroxisomes without coupling to ATP production: acyl-CoA
 417 oxidase catalyzes the oxidation of FADH₂ with electron transfer to O₂; amino acid oxidases oxidize
 418 flavin mononucleotide FMNH₂ or FADH₂ (**Figure 2A**).

419



420
421
422
423
424
425
426
427
428
429

430 (B) Respiration in mitochondrial preparations: The mitochondrial electron transfer system
 431 (ETS) is (1) fuelled by diffusion and transport of substrates across the mtOM and mtIM,
 432 and in addition consists of the (2) matrix-ETS, and (3) membrane-ETS. Electron transfer
 433 converges at the N-junction, and from CI, CII and electron transferring flavoprotein
 434 complex (CETF) at the Q-junction. Unlabeled arrows converging at the Q-junction indicate
 435 additional ETS-sections with electron entry into Q through glycerophosphate
 436 dehydrogenase, dihydroorotate dehydrogenase, proline dehydrogenase, choline
 437 dehydrogenase, and sulfide-ubiquinone oxidoreductase. The dotted arrow indicates the
 438 branched pathway of oxygen consumption by alternative quinol oxidase (AOX). ET-
 439 pathways are coupled to the phosphorylation-pathway. The H^+_{pos}/O_2 ratio is the outward
 440 proton flux from the matrix space to the positively (pos) charged vesicular compartment,
 441 divided by catabolic O_2 flux in the NADH-pathway. The H^+_{neg}/P_{\gg} ratio is the inward proton
 442 flux from the inter-membrane space to the negatively (neg) charged matrix space, divided
 443 by the flux of phosphorylation of ADP to ATP. These stoichiometries are not fixed because
 444 of ion leaks and proton slip. Modified from Lemieux *et al.* (2017) and Rich (2013).
 445 (C) OXPHOS coupling: O_2 flux through the catabolic ET-pathway, J_{kO_2} , is coupled
 446 by the H^+ circuit to flux through the phosphorylation-pathway of ADP to ATP, $J_{P_{\gg}}$.
 447 (D) Phosphorylation-pathway catalyzed by the proton pump F_1F_0 -ATPase (F-ATPase,
 448 ATP synthase), adenine nucleotide translocase (ANT), and inorganic phosphate carrier
 449 (PiC). The H^+_{neg}/P_{\gg} stoichiometry is the sum of the coupling stoichiometry in the F-ATPase
 450 reaction ($-2.7 H^+_{\text{pos}}$ from the positive intermembrane space, $2.7 H^+_{\text{neg}}$ to the matrix, *i.e.*, the
 451 negative compartment) and the proton balance in the translocation of ADP^{3-} , ATP^{4-} and P_i^{2-}
 452 (negative for substrates). Modified from Gnaiger (2014).
 453

454 The plasma membrane separates the intracellular compartment including the cytosol, nucleus, and
 455 organelles from the extracellular environment. The plasma membrane consists of a lipid bilayer with
 456 embedded proteins and attached organic molecules that collectively control the selective permeability
 457 of ions, organic molecules, and particles across the cell boundary. The intact plasma membrane prevents
 458 the passage of many water-soluble mitochondrial substrates and inorganic ions—such as succinate,
 459 adenosine diphosphate (ADP) and inorganic phosphate (P_i) that must be precisely controlled at
 460 kinetically-saturating concentrations for the analysis of mitochondrial respiratory capacities.
 461 Respiratory capacities delineate, comparable to channel capacity in information theory (Schneider
 462 2006), the upper boundary of the rate of O_2 consumption measured in defined respiratory states. Despite
 463 the activity of solute carriers, *e.g.*, the sodium-dependent dicarboxylate transporter SLC13A3 and the
 464 sodium-dependent phosphate transporter SLC20A2, which transport specific metabolites across the
 465 plasma membrane of various cell types, the intact plasma membrane limits the scope of investigations
 466 into mitochondrial respiratory function in intact cells.

467 **2.1.2. Specification of biochemical dose:** Substrates, uncouplers, inhibitors, and other chemical
 468 reagents are titrated to analyse cellular and mitochondrial function. Nominal concentrations of these
 469 substances are usually reported as initial amount of substance concentration [$\text{mol}\cdot\text{L}^{-1}$] in the incubation
 470 medium. When aiming at the measurement of kinetically saturated processes—such as OXPHOS-
 471 capacities—the concentrations for substrates can be chosen according to the apparent equilibrium
 472 constant, K_m' . In the case of hyperbolic kinetics, only 80% of maximum respiratory capacity is obtained
 473 at a substrate concentration of four times the K_m' , whereas substrate concentrations of 5, 9, 19 and 49
 474 times the K_m' are theoretically required for reaching 83%, 90%, 95% or 98% of the maximal rate
 475 (Gnaiger 2001). Other reagents are chosen to inhibit or alter a particular process. The amount of these
 476 chemicals in an experimental incubation is selected to maximize effect, avoiding unacceptable off-target
 477 consequences that would adversely affect the data being sought. Specifying the amount of substance in
 478 an incubation as nominal concentration in the aqueous incubation medium can be ambiguous (Doskey
 479 *et al.* 2015), particularly for cations (TPP⁺; fluorescent dyes such as safranin, TMRM; Chowdhury *et al.*
 480 2015) and lipophilic substances (oligomycin, uncouplers, permeabilization agents; Doerrier *et al.* 2018),
 481 which accumulate in the mitochondrial matrix or in biological membranes, respectively. Generally,
 482 dose/exposure can be specified per unit of biological sample, *i.e.*, (nominal moles of
 483 xenobiotic)/(number of cells) [$\text{mol}\cdot\text{cell}^{-1}$] or, as appropriate, per mass of biological sample [$\text{mol}\cdot\text{kg}^{-1}$].
 484 This approach to specification of dose/exposure provides a scalable parameter that can be used to design

485 experiments, help interpret a wide variety of experimental results, and provide absolute information that
 486 allows researchers worldwide to make the most use of published data (Doskey *et al.* 2015).

487

488 2.2. Mitochondrial preparations

489

490 Mitochondrial preparations are defined as either isolated mitochondria or tissue and cellular
 491 preparations in which the barrier function of the plasma membrane is disrupted. Since this entails the
 492 loss of cell viability, mitochondrial preparations are not studied *in vivo*. In contrast to isolated
 493 mitochondria and tissue homogenate preparations, mitochondria in permeabilized tissues and cells are
 494 *in situ* relative to the plasma membrane. When studying mitochondrial preparations, substrate-
 495 uncoupler-inhibitor-titration (SUIT) protocols are used to establish respiratory coupling control states
 496 (CCS) and pathway control states (PCS) that provide reference values for various output variables
 497 (Table 1). Physiological conditions *in vivo* deviate from these experimentally obtained states; this is
 498 because kinetically-saturating concentrations, *e.g.*, of ADP, oxygen (O₂; dioxygen) or fuel substrates,
 499 may not apply to physiological intracellular conditions. Further information is obtained in studies of
 500 kinetic responses to variations in fuel substrate concentrations, [ADP], or [O₂] in the range between
 501 kinetically-saturating concentrations and anoxia (Gnaiger 2001).

502 The cholesterol content of the plasma membrane is high compared to mitochondrial membranes
 503 (Korn 1969). Therefore, mild detergents—such as digitonin and saponin—can be applied to selectively
 504 permeabilize the plasma membrane via interaction with cholesterol; this allows free exchange of organic
 505 molecules and inorganic ions between the cytosol and the immediate cell environment, while
 506 maintaining the integrity and localization of organelles, cytoskeleton, and the nucleus. Application of
 507 permeabilization agents (mild detergents or toxins) leads to washout of cytosolic marker enzymes—
 508 such as lactate dehydrogenase—and results in the complete loss of cell viability (tested by nuclear
 509 staining using plasma membrane-impermeable dyes), while mitochondrial function remains intact
 510 (tested by cytochrome *c* stimulation of respiration). Digitonin concentrations have to be optimized
 511 according to cell type, particularly since mitochondria from cancer cells contain significantly higher
 512 contents of cholesterol in both membranes (Baggetto and Testa-Perussini, 1990). For example, a dose
 513 of digitonin of 8 fmol·cell⁻¹ (10 pg·cell⁻¹; 10 μg·10⁻⁶ cells) is optimal for permeabilization of endothelial
 514 cells, and the concentration in the incubation medium has to be adjusted according to the cell density
 515 (Doerrier *et al.* 2018). Respiration of isolated mitochondria remains unaltered after the addition of low
 516 concentrations of digitonin or saponin. In addition to mechanical cell disruption during homogenization
 517 of tissue, permeabilization agents may be applied to ensure permeabilization of all cells in tissue
 518 homogenates.

519 Suspensions of cells permeabilized in the respiration chamber and crude tissue homogenates
 520 contain all components of the cell at highly dilute concentrations. All mitochondria are retained in
 521 chemically-permeabilized mitochondrial preparations and crude tissue homogenates. In the preparation
 522 of isolated mitochondria, however, the mitochondria are separated from other cell fractions and purified
 523 by differential centrifugation, entailing the loss of mitochondria at typical recoveries ranging from 30%
 524 to 80% of total mitochondrial content (Lai *et al.* 2018). Using Percoll or sucrose density gradients to
 525 maximize the purity of isolated mitochondria may compromise the mitochondrial yield or structural and
 526 functional integrity. Therefore, mitochondrial isolation protocols need to be optimized according to each
 527 study. The term, *mitochondrial preparation*, neither includes intact cells, nor submitochondrial particles
 528 and further fractionated mitochondrial components.

529

530 2.3. Electron transfer pathways

531

532 Mitochondrial electron transfer (ET) pathways are fuelled by diffusion and transport of substrates
 533 across the mtOM and mtIM. In addition, the mitochondrial electron transfer system (ETS) consists of
 534 the matrix-ETS and membrane-ETS (Figure 2B). Upstream sections of ET-pathways converge at the
 535 NADH-junction (N-junction). NADH is mainly generated in the tricarboxylic acid (TCA) cycle and is
 536 oxidized by Complex I (CI), with further electron entry into the coenzyme Q-junction (Q-junction).
 537 Similarly, succinate is formed in the TCA cycle and oxidized by CII to fumarate. CII is part of both the
 538 TCA cycle and the ETS, and reduces FAD to FADH₂ with further reduction of ubiquinone to ubiquinol
 539 downstream of the TCA cycle in the Q-junction. Thus FADH₂ is not a substrate but is the product of
 540 CII, in contrast to erroneous metabolic maps shown in many publications. β-oxidation of fatty acids

541 (FA) supplies reducing equivalents via (1) FADH₂ as the substrate of electron transferring flavoprotein
 542 complex (CETF); (2) acetyl-CoA generated by chain shortening; and (3) NADH generated via 3-
 543 hydroxyacyl-CoA dehydrogenases. The ATP yield depends on whether acetyl-CoA enters the TCA
 544 cycle, or is for example used in ketogenesis.

545 Selected mitochondrial catabolic pathways, *k*, of electron transfer from the oxidation of fuel
 546 substrates to the reduction of O₂ are activated by addition of fuel substrates to the mitochondrial
 547 respiration medium after depletion of endogenous substrates (**Figure 2B**). Substrate combinations and
 548 specific inhibitors of ET-pathway enzymes are used to obtain defined pathway control states in
 549 mitochondrial preparations (Gnaiger 2014).

550

551 2.4. Respiratory coupling control

552

553 **2.4.1. Coupling:** In mitochondrial electron transfer, vectorial transmembrane proton flux is
 554 coupled through the redox proton pumps CI, CIII and CIV to the catabolic flux of scalar reactions,
 555 collectively measured as O₂ flux, J_{kO_2} (**Figure 2**). Thus mitochondria are elementary components of
 556 energy transformation. Energy is a conserved quantity and cannot be lost or produced in any internal
 557 process (First Law of Thermodynamics). Open and closed systems can gain or lose energy only by
 558 external fluxes—by exchange with the environment. Therefore, energy can neither be produced by
 559 mitochondria, nor is there any internal process without energy conservation. Exergy or Gibbs energy
 560 (‘free energy’) is the part of energy that can potentially be transformed into work under conditions of
 561 constant temperature and pressure. *Coupling* is the interaction of an exergonic process (spontaneous,
 562 negative exergy change) with an endergonic process (positive exergy change) in energy transformations
 563 which conserve part of the exergy that would be irreversibly lost or dissipated in an uncoupled process.

564 Pathway control states (PCS) and coupling control states (CCS) are complementary, since
 565 mitochondrial preparations depend on (1) an exogenous supply of pathway-specific fuel substrates and
 566 oxygen, and (2) exogenous control of phosphorylation (**Figure 2**).

567 **2.4.2. Phosphorylation, P_», and P_»/O₂ ratio:** Phosphorylation in the context of OXPHOS is
 568 defined as phosphorylation of ADP by P_i to form ATP. On the other hand, the term phosphorylation is
 569 used generally in many contexts, *e.g.*, protein phosphorylation. This justifies consideration of a symbol
 570 more discriminating and specific than P as used in the P/O ratio (phosphate to atomic oxygen ratio),
 571 where P indicates phosphorylation of ADP to ATP or GDP to GTP (**Figure 2**). We propose the symbol
 572 P_» for the endergonic (uphill) direction of phosphorylation ADP→ATP, and likewise the symbol P_« for
 573 the corresponding exergonic (downhill) hydrolysis ATP→ADP. P_» refers mainly to electrontransfer
 574 phosphorylation but may also involve substrate-level phosphorylation as part of the TCA cycle
 575 (succinyl-CoA ligase, phosphoglycerate kinase) and phosphorylation of ADP catalyzed by pyruvate
 576 kinase, and of GDP phosphorylated by phosphoenolpyruvate carboxykinase. Transphosphorylation is
 577 performed by adenylate kinase, creatine kinase (mtCK), hexokinase and nucleoside diphosphate kinase.
 578 In isolated mammalian mitochondria, ATP production catalyzed by adenylate kinase (2 ADP ↔ ATP +
 579 AMP) proceeds without fuel substrates in the presence of ADP (Kömllódi and Tretter 2017). Kinase
 580 cycles are involved in intracellular energy transfer and signal transduction for regulation of energy flux.

581 The P_»/O₂ ratio (P_»/4 e⁻) is two times the ‘P/O’ ratio (P_»/2 e⁻). P_»/O₂ is a generalized symbol, not
 582 specific for reporting P_i consumption (P_i/O₂ flux ratio), ADP depletion (ADP/O₂ flux ratio), or ATP
 583 production (ATP/O₂ flux ratio). The mechanistic P_»/O₂ ratio—or P_»/O₂ stoichiometry—is calculated
 584 from the proton-to-O₂ and proton-to-phosphorylation coupling stoichiometries (**Figure 2B**):

$$586 \quad P_{\gg}/O_2 = \frac{H_{p_{\text{pos}}/O_2}^+}{H_{n_{\text{neg}}/P_{\gg}}^+} \quad (1)$$

587

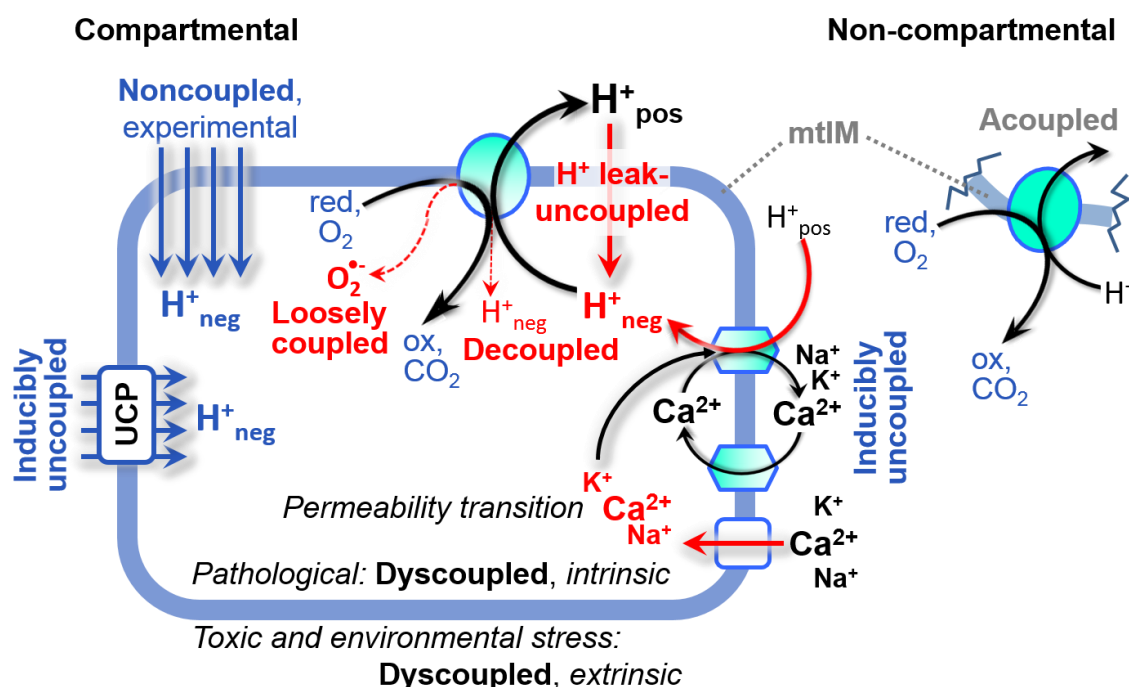
588 The H⁺_{pos}/O₂ coupling stoichiometry (referring to the full four electron reduction of O₂) depends on the
 589 relative involvement of the three coupling sites (respiratory Complexes CI, CIII and CIV) in the
 590 catabolic ET-pathway from reduced fuel substrates (electron donors) to the reduction of O₂ (electron
 591 acceptor). This varies with: (1) a bypass of CI by single or multiple electron input into the Q-junction;
 592 and (2) a bypass of CIV by involvement of alternative oxidases, AOX. AOX are expressed in all plants,
 593 some fungi, many protists, and several animal phyla, but are not expressed in vertebrate mitochondria
 594 (McDonald *et al.* 2009).

595 The H⁺_{pos}/O₂ coupling stoichiometry equals 12 in the ET-pathways involving CIII and CIV as
 596 proton pumps, increasing to 20 for the NADH-pathway through CI (**Figure 2B**), but a general consensus
 597 on H⁺_{pos}/O₂ stoichiometries remains to be reached (Hinkle 2005; Wikström and Hummer 2012; Sazanov

598 2015). The H^+_{neg}/P_{\gg} coupling stoichiometry (3.7; **Figure 2B**) is the sum of 2.7 H^+_{neg} required by the F-
 599 ATPase of vertebrate and most invertebrate species (Watt *et al.* 2010) and the proton balance in the
 600 translocation of ADP, ATP and P_i (**Figure 2C**). Taken together, the mechanistic P_{\gg}/O_2 ratio is calculated
 601 at 5.4 and 3.3 for NADH- and succinate-linked respiration, respectively (Eq. 1). The corresponding
 602 classical P_{\gg}/O ratios (referring to the 2 electron reduction of $0.5 O_2$) are 2.7 and 1.6 (Watt *et al.* 2010),
 603 in agreement with the measured P_{\gg}/O ratio for succinate of 1.58 ± 0.02 (Gnaiger *et al.* 2000).

604 **2.4.3. Uncoupling:** The effective P_{\gg}/O_2 flux ratio ($Y_{P_{\gg}/O_2} = J_{P_{\gg}}/J_{K_{O_2}}$) is diminished relative to the
 605 mechanistic P_{\gg}/O_2 ratio by intrinsic and extrinsic uncoupling or dyscoupling (**Figure 3**). Such
 606 generalized uncoupling is different from switching to mitochondrial pathways that involve fewer than
 607 three proton pumps ('coupling sites': Complexes CI, CIII and CIV), bypassing CI through multiple
 608 electron entries into the Q-junction, or CIII and CIV through AOX (**Figure 2B**). Reprogramming of
 609 mitochondrial pathways leading to different types of substrates being oxidized may be considered as a
 610 switch of gears (changing the stoichiometry by altering the substrate that is oxidized) rather than
 611 uncoupling (loosening the tightness of coupling relative to a fixed stoichiometry). In addition, Y_{P_{\gg}/O_2}
 612 depends on several experimental conditions of flux control, increasing as a hyperbolic function of [ADP]
 613 to a maximum value (Gnaiger 2001).

614



615

616

Figure 3. Mechanisms of respiratory uncoupling

617 An intact mitochondrial inner membrane, mtIM, is required for vectorial, compartmental coupling.
 618 'Acoupled' respiration is the consequence of structural disruption with catalytic activity of non-
 619 compartmental mitochondrial fragments. Inducible uncoupling, *e.g.*, by activation of UCP1, increases
 620 LEAK-respiration; experimentally noncoupled respiration provides an estimate of ET-capacity obtained
 621 by titration of protonophores stimulating respiration to maximum O_2 flux. H^+ leak-uncoupled,
 622 decoupled, and loosely coupled respiration are components of intrinsic uncoupling (**Table 2**).
 623 Pathological dysfunction may affect all types of uncoupling, including permeability transition (mtPT),
 624 causing intrinsically dyscoupled respiration. Similarly, toxicological and environmental stress factors
 625 can cause extrinsically dyscoupled respiration. Reduced fuel substrates, red; oxidized products, ox.
 626

627 Uncoupling of mitochondrial respiration is a general term comprising diverse mechanisms:

- 628 1. Proton leak across the mtIM from the positive to the negative compartment (H^+ leak-uncoupled;
 629 **Figure 3**).
- 630 2. Cycling of other cations, strongly stimulated by mtPT; comparable to the use of protonophores,
 631 cation cycling is experimentally induced by valinomycin in the presence of K^+ ;
- 632 3. Decoupling by proton slip in the redox proton pumps when protons are effectively not pumped
 633 (CI, CIII and CIV) or are not driving phosphorylation (F-ATPase);

- 634 4. Loss of vesicular (compartmental) integrity when electron transfer is acoupled;
 635 5. Electron leak in the loosely coupled univalent reduction of O₂ to superoxide (O₂^{•-}; superoxide
 636 anion radical).

637 Differences of terms—uncoupled *vs.* noncoupled—are easily overlooked, although they relate to
 638 different meanings of uncoupling (**Figure 3** and **Table 2**).

639

640 2.5. Coupling states and respiratory rates

641

642 To extend the classical nomenclature on mitochondrial coupling states (Section 2.6) by a concept-
 643 driven terminology that explicitly incorporates information on the meaning of respiratory states, the
 644 terminology must be general and not restricted to any particular experimental protocol or mitochondrial
 645 preparation (Gnaiger 2009). Concept-driven nomenclature aims at mapping the meaning and concept
 646 behind the words and acronyms onto the forms of words and acronyms (Miller 1991). The focus of
 647 concept-driven nomenclature is primarily the conceptual *why*, along with clarification of the
 648 experimental *how*.

649

650 **Table 1. Coupling states and residual oxygen consumption in mitochondrial**
 651 **preparations in relation to respiration- and phosphorylation-flux, J_{KO_2} and J_{P} , and**
 652 **protonmotive force, pmf.** Coupling states are established at kinetically-saturating
 653 concentrations of fuel substrates and O₂.

State	J_{KO_2}	J_{P}	pmf	Inducing factors	Limiting factors
LEAK	<i>L</i> ; low, cation leak-dependent respiration	0	max.	back-flux of cations including proton leak, proton slip	$J_{\text{P}} = 0$: (1) without ADP, L_{N} ; (2) max. ATP/ADP ratio, L_{T} ; or (3) inhibition of the phosphorylation-pathway, L_{Omy}
OXPHOS	<i>P</i> ; high, ADP-stimulated respiration, OXPHOS-capacity	max.	high	kinetically-saturating [ADP] and [P _i]	J_{P} by phosphorylation-pathway capacity; or J_{KO_2} by ET-capacity
ET	<i>E</i> ; max., noncoupled respiration, ET-capacity	0	low	optimal external uncoupler concentration for max. $J_{\text{O}_2, \text{E}}$	J_{KO_2} by ET-capacity
ROX	<i>Rox</i> ; min., residual O ₂ consumption	0	0	$J_{\text{O}_2, \text{Rox}}$ in non-ET-pathway oxidation reactions	inhibition of all ET-pathways; or absence of fuel substrates

654

655 To provide a diagnostic reference for respiratory capacities of core energy metabolism, the
 656 capacity of oxidative phosphorylation, OXPHOS, is measured at kinetically-saturating concentrations
 657 of ADP and P_i. The oxidative ET-capacity reveals the limitation of OXPHOS-capacity mediated by the
 658 phosphorylation-pathway. The ET- and phosphorylation-pathways comprise coupled segments of the
 659 OXPHOS-system. By application of external uncouplers, ET-capacity is measured as noncoupled
 660 respiration. The contribution of intrinsically uncoupled O₂ consumption is studied by preventing the
 661 stimulation of phosphorylation either in the absence of ADP or by inhibition of the phosphorylation-
 662 pathway. The corresponding states are collectively classified as LEAK-states when O₂ consumption
 663 compensates mainly for ion leaks, including the proton leak. Defined coupling states are induced by: (1)
 664 adding cation chelators such as EGTA, binding free Ca²⁺ and thus limiting cation cycling; (2) adding
 665 ADP and P_i; (3) inhibiting the phosphorylation-pathway; and (4) uncoupler titrations, while maintaining
 666 a defined ET-pathway state with constant fuel substrates and inhibitors of specific branches of the ET-
 667 pathway.

668 The three coupling states, ET, LEAK and OXPHOS, are shown schematically with the
 669 corresponding respiratory rates, abbreviated as *E*, *L* and *P*, respectively (**Figure 4**). We distinguish

670 metabolic *pathways* from metabolic *states* and the corresponding metabolic *rates*; for example: ET-
 671 pathways, ET-states, and ET-capacities, E , respectively (**Table 1**). The protonmotive force is *high* in
 672 the OXPPOS-state when it drives phosphorylation, *maximum* in the LEAK-state of coupled
 673 mitochondria, driven by LEAK-respiration at a minimum back-flux of cations to the matrix side, and
 674 *very low* in the ET-state when uncouplers short-circuit the proton cycle (**Table 1**).

675

676 **Figure 4. Four-compartment**
 677 **model of oxidative**
 678 **phosphorylation**

679 Respiratory states (ET, OXPPOS,
 680 LEAK; **Table 1**) and corresponding
 681 rates (E , P , L) are connected by the
 682 protonmotive force, pmf. (1) ET-
 683 capacity, E , is partitioned into (2)
 684 dissipative LEAK-respiration, L ,
 685 when the Gibbs energy change of
 686 catabolic O_2 flux is irreversibly lost,
 687 (3) net OXPPOS-capacity, $P-L$, with
 688 partial conservation of the capacity to perform work, and (4) the excess capacity, $E-P$. Modified from
 689 Gnaiger (2014).

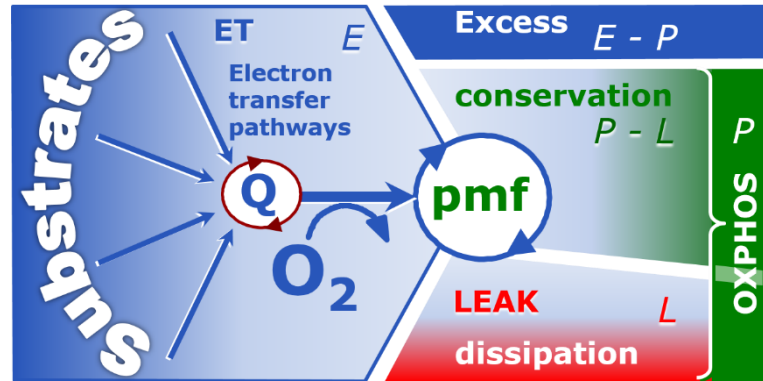
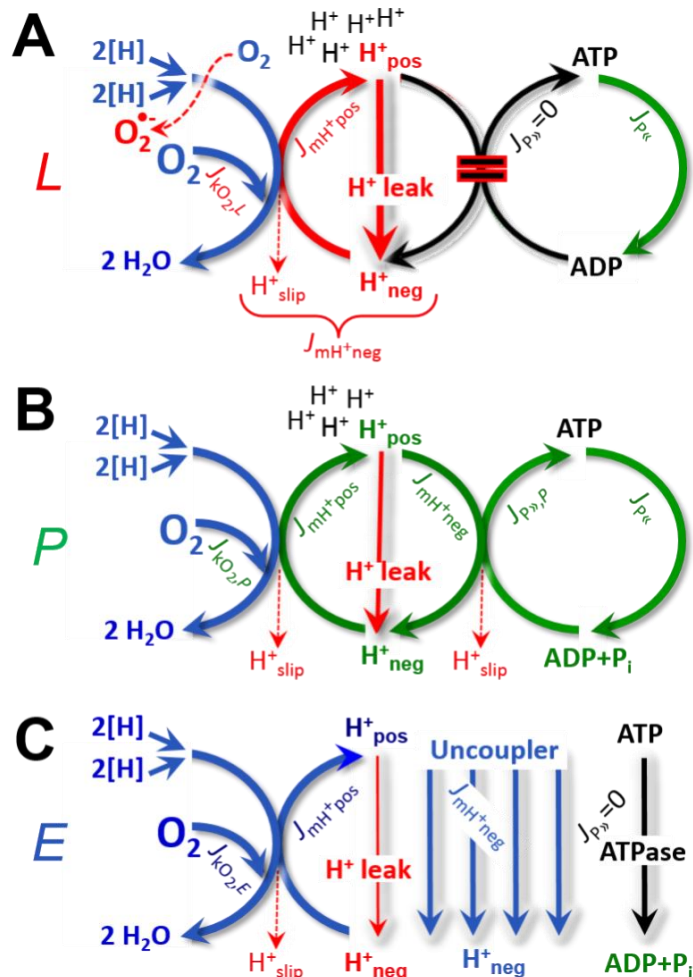


Figure 5. Respiratory coupling states

(A) **LEAK-state and rate, L** : Oxidation only, since phosphorylation is arrested, $J_{P\gg} = 0$, and catabolic O_2 flux, $J_{kO_2,L}$, is controlled mainly by the proton leak and slip, J_{mH^+neg} , at maximum protonmotive force (**Figure 4**). Extramitochondrial ATP may be hydrolyzed by extramitochondrial ATPases, $J_{P\ll}$; then phosphorylation must be blocked.

(B) **OXPPOS-state and rate, P** : Oxidation coupled to phosphorylation, $J_{P\gg}$, which is stimulated by kinetically-saturating [ADP] and $[P_i]$, supported by a high protonmotive force. O_2 flux, $J_{kO_2,P}$, is well-coupled at a $P\gg/O_2$ flux ratio of $J_{P\gg,P} \cdot J_{O_2,P}^{-1}$. Extramitochondrial ATPases may recycle ATP, $J_{P\ll}$.

(C) **ET-state and rate, E** : Oxidation only, since phosphorylation is zero, $J_{P\gg} = 0$, at optimum exogenous uncoupler concentration when noncoupled respiration, $J_{kO_2,E}$, is maximum. The F-ATPase may hydrolyze extramitochondrial ATP.



690

691

692 **2.5.1. LEAK-state (Figure 5A)**: The LEAK-state is defined as a state of mitochondrial
 693 respiration when O_2 flux mainly compensates for ion leaks in the absence of ATP synthesis, at
 kinetically-saturating concentrations of O_2 , respiratory fuel substrates and P_i . LEAK-respiration is

694 measured to obtain an estimate of intrinsic uncoupling without addition of an experimental uncoupler:
 695 (1) in the absence of adenylates, *i.e.*, AMP, ADP and ATP; (2) after depletion of ADP at a maximum
 696 ATP/ADP ratio; or (3) after inhibition of the phosphorylation-pathway by inhibitors of F-ATPase—such
 697 as oligomycin, or of adenine nucleotide translocase—such as carboxyatractyloside. Adjustment of the
 698 nominal concentration of these inhibitors to the density of biological sample applied can minimize or
 699 avoid inhibitory side-effects exerted on ET-capacity or even some dyscoupling.

700

701 **Table 2. Terms on respiratory coupling and uncoupling.**

Term	J_{kO_2}	$P \gg O_2$	Notes	
acoupled		0	electron transfer in mitochondrial fragments without vectorial proton translocation (Figure 3)	
intrinsic, no protonophore added	uncoupled	L	0	non-phosphorylating LEAK-respiration (Figure 5A)
	proton leak-uncoupled		0	component of L , H^+ diffusion across the mtIM (Figure 3)
	decoupled		0	component of L , proton slip (Figure 3)
	loosely coupled		0	component of L , lower coupling due to superoxide formation and bypass of proton pumps by electron leak (Figure 3)
	dyscoupled		0	pathologically, toxicologically, environmentally increased uncoupling, mitochondrial dysfunction
	inducibly uncoupled		0	by UCP1 or cation (<i>e.g.</i> , Ca^{2+}) cycling (Figure 3)
noncoupled	E	0	ET-capacity, non-phosphorylating respiration stimulated to maximum flux at optimum exogenous protonophore concentration (Figure 5C)	
well-coupled	P	high	OXPPOS-capacity , phosphorylating respiration with an intrinsic LEAK component (Figure 5B)	
fully coupled	$P - L$	max.	OXPPOS-capacity corrected for LEAK-respiration (Figure 4)	

702

703

704

705

706

707

708

709

710

711

712

713

714

715

716

717

718

719

720

721

722

- **Proton leak and uncoupled respiration:** The intrinsic proton leak is the *uncoupled* leak current of protons in which protons diffuse across the mtIM in the dissipative direction of the downhill protonmotive force without coupling to phosphorylation (**Figure 5A**). The proton leak flux depends non-linearly on the protonmotive force (Garlid *et al.* 1989; Divakaruni and Brand 2011), which is a temperature-dependent property of the mtIM and may be enhanced due to possible contamination by free fatty acids. Inducible uncoupling mediated by uncoupling protein 1 (UCP1) is physiologically controlled, *e.g.*, in brown adipose tissue. UCP1 is a member of the mitochondrial carrier family that is involved in the translocation of protons across the mtIM (Jezek *et al.* 2018). Consequently, this short-circuit lowers the protonmotive force and stimulates electron transfer, respiration, and heat dissipation in the absence of phosphorylation of ADP.
- **Cation cycling:** There can be other cation contributors to leak current including calcium and probably magnesium. Calcium influx is balanced by mitochondrial Na^+/Ca^{2+} or H^+/Ca^{2+} exchange, which is balanced by Na^+/H^+ or K^+/H^+ exchanges. This is another effective uncoupling mechanism different from proton leak (**Table 2**).
- **Proton slip and decoupled respiration:** Proton slip is the *decoupled* process in which protons are only partially translocated by a redox proton pump of the ET-pathways and slip back to the original vesicular compartment. The proton leak is the dominant contributor to the overall leak current in mammalian mitochondria incubated under physiological conditions at 37 °C, whereas proton slip increases at lower experimental temperature (Canton *et al.* 1995). Proton slip can also happen in association with the F-ATPase, in which the proton slips downhill across the pump to

723 the matrix without contributing to ATP synthesis. In each case, proton slip is a property of the
724 proton pump and increases with the pump turnover rate.

- 725 • **Electron leak and loosely coupled respiration:** Superoxide production by the ETS leads to a
726 bypass of redox proton pumps and correspondingly lower P_{\gg}/O_2 ratio. This depends on the actual
727 site of electron leak and the scavenging of hydrogen peroxide by cytochrome *c*, whereby electrons
728 may re-enter the ETS with proton translocation by CIV.
- 729 • **Loss of compartmental integrity and acoupled respiration:** Electron transfer and catabolic O_2
730 flux proceed without compartmental proton translocation in disrupted mitochondrial fragments.
731 Such fragments are an artefact of mitochondrial isolation, and may not fully fuse to re-establish
732 structurally intact mitochondria. Loss of mtIM integrity, therefore, is the cause of acoupled
733 respiration, which is a nonvectorial dissipative process without control by the protonmotive force.
- 734 • **Dyscoupled respiration:** Mitochondrial injuries may lead to *dyscoupling* as a pathological or
735 toxicological cause of *uncoupled* respiration. Dyscoupling may involve any type of uncoupling
736 mechanism, *e.g.*, opening the mtPT pore. Dyscoupled respiration is distinguished from the
737 experimentally induced *noncoupled* respiration in the ET-state (**Table 2**).

738
739 **2.5.2. OXPHOS-state (Figure 5B):** The OXPHOS-state is defined as the respiratory state with
740 kinetically-saturating concentrations of O_2 , respiratory and phosphorylation substrates, and absence of
741 exogenous uncoupler, which provides an estimate of the maximal respiratory capacity in the OXPHOS-
742 state for any given ET-pathway state. Respiratory capacities at kinetically-saturating substrate
743 concentrations provide reference values or upper limits of performance, aiming at the generation of data
744 sets for comparative purposes. Physiological activities and effects of substrate kinetics can be evaluated
745 relative to the OXPHOS-capacity.

746 As discussed previously, 0.2 mM ADP does not fully saturate flux in isolated mitochondria
747 (Gnaiger 2001; Puchowicz *et al.* 2004); greater [ADP] is required, particularly in permeabilized muscle
748 fibres and cardiomyocytes, to overcome limitations by intracellular diffusion and by the reduced
749 conductance of the mtOM (Jepihhina *et al.* 2011; Illaste *et al.* 2012; Simson *et al.* 2016), either through
750 interaction with tubulin (Rostovtseva *et al.* 2008) or other intracellular structures (Birkedal *et al.* 2014).
751 In addition, saturating ADP concentrations need to be evaluated under different experimental conditions
752 such as temperature (Lemieux *et al.* 2017) and with different animal models (Blier and Guderley, 1993).
753 In permeabilized muscle fibre bundles of high respiratory capacity, the apparent K_m for ADP increases
754 up to 0.5 mM (Saks *et al.* 1998), consistent with experimental evidence that >90% saturation is reached
755 only at >5 mM ADP (Pesta and Gnaiger 2012). Similar ADP concentrations are also required for
756 accurate determination of OXPHOS-capacity in human clinical cancer samples and permeabilized cells
757 (Klepinin *et al.* 2016; Koit *et al.* 2017). 2.5 to 5 mM ADP is sufficient to obtain the actual OXPHOS-
758 capacity in many types of permeabilized tissue and cell preparations, but experimental validation is
759 required in each specific case.

760 **2.5.3. Electron transfer-state (Figure 5C):** O_2 flux determined in the ET-state yields an estimate
761 of ET-capacity. The ET-state is defined as the *noncoupled* state with kinetically-saturating
762 concentrations of O_2 , respiratory substrate and optimum exogenous uncoupler concentration for
763 maximum O_2 flux. Uncouplers are weak lipid-soluble acids which function as protonophores. These
764 disrupt the barrier function of the mtIM and thus short circuit the protonmotive system, functioning like
765 a clutch in a mechanical system. As a consequence of the nearly collapsed protonmotive force, the
766 driving force is insufficient for phosphorylation, and $J_{P_{\gg}} = 0$. The most frequently used uncouplers are
767 carbonyl cyanide *m*-chloro phenyl hydrazone (CCCP), carbonyl cyanide *p*-
768 trifluoromethoxyphenylhydrazone (FCCP), or dinitrophenol (DNP). Stepwise titration of uncouplers
769 stimulates respiration up to or above the level of O_2 consumption rates in the OXPHOS-state; respiration
770 is inhibited, however, above optimum uncoupler concentrations (Mitchell 2011). Data obtained with a
771 single dose of uncoupler must be evaluated with caution, particularly when a fixed uncoupler
772 concentration is used in studies exploring a treatment or disease that may alter the mitochondrial content
773 or mitochondrial sensitivity to inhibition by uncouplers. There is a need for new protonophoric
774 uncouplers that drive maximal respiration across a broad dosing range and do not inhibit respiration at
775 high concentrations (Kenwood *et al.* 2013). The effect on ET-capacity of the reversed function of F-
776 ATPase ($J_{P_{\ll}}$; **Figure 5C**) can be evaluated in the presence and absence of extramitochondrial ATP.

777 **2.5.4. ROX state and Rox:** Besides the three fundamental coupling states of mitochondrial
778 preparations, the state of residual O_2 consumption, ROX, which although not a coupling state, is relevant

779 to assess respiratory function (**Figure 1**). The rate of residual oxygen consumption, *Rox*, is defined as
 780 O₂ consumption due to oxidative reactions measured after inhibition of ET with rotenone, malonic acid
 781 and antimycin A. Cyanide and azide inhibit not only CIV but catalase and several peroxidases involved
 782 in *Rox*. High concentrations of antimycin A, but not rotenone or cyanide, inhibit peroxisomal acyl-CoA
 783 oxidase and D-amino acid oxidase (Vamecq *et al.* 1987). *Rox* represents a baseline used to correct
 784 respiration measured in defined coupling control states. *Rox*-corrected *L*, *P* and *E* not only lower the
 785 values of total fluxes, but also change the flux control ratios *L/P* and *L/E*. *Rox* is not necessarily
 786 equivalent to non-mitochondrial reduction of O₂, considering O₂-consuming reactions in mitochondria
 787 that are not related to ET—such as O₂ consumption in reactions catalyzed by monoamine oxidases (type
 788 A and B), monooxygenases (cytochrome P450 monooxygenases), dioxygenase (sulfur dioxygenase and
 789 trimethyllysine dioxygenase), and several hydroxylases. Even isolated mitochondrial fractions,
 790 especially those obtained from liver, may be contaminated by peroxisomes, as shown by transmission
 791 electron microscopy. This fact makes the exact determination of mitochondrial O₂ consumption and
 792 mitochondria-associated generation of reactive oxygen species complicated (Schönfeld *et al.* 2009;
 793 Speijer 2016; **Figure 2**). The dependence of ROX-linked O₂ consumption needs to be studied in detail
 794 together with non-ET enzyme activities, availability of specific substrates, O₂ concentration, and
 795 electron leakage leading to the formation of reactive oxygen species.

796 **2.5.5. Quantitative relations:** *E* may exceed or be equal to *P*. $E > P$ is observed in many types
 797 of mitochondria, varying between species, tissues and cell types (Gnaiger 2009). *E-P* is the excess ET-
 798 capacity pushing the phosphorylation-flux (**Figure 2C**) to the limit of its capacity for utilizing the
 799 protonmotive force. In addition, the magnitude of *E-P* depends on the tightness of respiratory coupling
 800 or degree of uncoupling, since an increase of *L* causes *P* to increase towards the limit of *E*. The *excess*
 801 *E-P* capacity, *E-P*, therefore, provides a sensitive diagnostic indicator of specific injuries of the
 802 phosphorylation-pathway, under conditions when *E* remains constant but *P* declines relative to controls
 803 (**Figure 4**). Substrate cocktails supporting simultaneous convergent electron transfer to the Q-junction
 804 for reconstitution of TCA cycle function establish pathway control states with high ET-capacity, and
 805 consequently increase the sensitivity of the *E-P* assay.

806 *E* cannot theoretically be lower than *P*. $E < P$ must be discounted as an artefact, which may be
 807 caused experimentally by: (1) loss of oxidative capacity during the time course of the respirometric
 808 assay, since *E* is measured subsequently to *P*; (2) using insufficient uncoupler concentrations; (3) using
 809 high uncoupler concentrations which inhibit ET (Gnaiger 2008); (4) high oligomycin concentrations
 810 applied for measurement of *L* before titrations of uncoupler, when oligomycin exerts an inhibitory effect
 811 on *E*. On the other hand, the excess ET-capacity is overestimated if non-saturating [ADP] or [P_i] are
 812 used. See State 3 in the next section.

813 The net OXPHOS-capacity is calculated by subtracting *L* from *P* (**Figure 4**). The net P_»/O₂ equals
 814 $P_{»}/(P-L)$, wherein the dissipative LEAK component in the OXPHOS-state may be overestimated. This
 815 can be avoided by measuring LEAK-respiration in a state when the protonmotive force is adjusted to its
 816 slightly lower value in the OXPHOS-state by titration of an ET inhibitor (Divakaruni and Brand 2011).
 817 Any turnover-dependent components of proton leak and slip, however, are underestimated under these
 818 conditions (Garlid *et al.* 1993). In general, it is inappropriate to use the term *ATP production* or *ATP*
 819 *turnover* for the difference of O₂ flux measured in the OXPHOS and LEAK states. *P-L* is the upper limit
 820 of OXPHOS-capacity that is freely available for ATP production (corrected for LEAK-respiration) and
 821 is fully coupled to phosphorylation with a maximum mechanistic stoichiometry (**Figure 4**).

822 LEAK-respiration and OXPHOS-capacity depend on (1) the tightness of coupling under the
 823 influence of the respiratory uncoupling mechanisms (**Figure 3**), and (2) the coupling stoichiometry,
 824 which varies as a function of the substrate type undergoing oxidation in ET-pathways with either two
 825 or three coupling sites (**Figure 2B**). When cocktails with NADH-linked substrates and succinate are
 826 used, the relative contribution of ET-pathways with three or two coupling sites cannot be controlled
 827 experimentally, is difficult to determine, and may shift in transitions between LEAK-, OXPHOS- and
 828 ET-states (Gnaiger 2014). Under these experimental conditions, we cannot separate the tightness of
 829 coupling *versus* coupling stoichiometry as the mechanisms of respiratory control in the shift of *L/P*
 830 ratios. The tightness of coupling and fully coupled O₂ flux, *P-L* (**Table 2**), therefore, are obtained from
 831 measurements of coupling control of LEAK-respiration, OXPHOS- and ET-capacities in well-defined
 832 pathway states, using either pyruvate and malate as substrates or the classical succinate and rotenone
 833 substrate-inhibitor combination (**Figure 2B**).

834 **2.5.6. The steady-state:** Mitochondria represent a thermodynamically open system in non-
 835 equilibrium states of biochemical energy transformation. State variables (protonmotive force; redox
 836 states) and metabolic *rates* (fluxes) are measured in defined mitochondrial respiratory *states*. Steady-
 837 states can be obtained only in open systems, in which changes by internal transformations, *e.g.*, O₂
 838 consumption, are instantaneously compensated for by external fluxes, *e.g.*, O₂ supply, preventing a
 839 change of O₂ concentration in the system (Gnaiger 1993b). Mitochondrial respiratory states monitored
 840 in closed systems satisfy the criteria of pseudo-steady states for limited periods of time, when changes
 841 in the system (concentrations of O₂, fuel substrates, ADP, P_i, H⁺) do not exert significant effects on
 842 metabolic fluxes (respiration, phosphorylation). Such pseudo-steady states require respiratory media
 843 with sufficient buffering capacity and substrates maintained at kinetically-saturating concentrations, and
 844 thus depend on the kinetics of the processes under investigation.
 845

846 2.6. Classical terminology for isolated mitochondria

847 *'When a code is familiar enough, it ceases appearing like a code; one forgets that there is a*
 848 *decoding mechanism. The message is identical with its meaning'* (Hofstadter 1979).
 849

850 Chance and Williams (1955; 1956) introduced five classical states of mitochondrial respiration
 851 and cytochrome redox states. **Table 3** shows a protocol with isolated mitochondria in a closed
 852 respirometric chamber, defining a sequence of respiratory states. States and rates are not specifically
 853 distinguished in this nomenclature.
 854

855 **Table 3. Metabolic states of mitochondria (Chance and**
 856 **Williams, 1956; Table V).**
 857

State	[O ₂]	ADP level	Substrate level	Respiration rate	Rate-limiting substance
1	>0	low	low	slow	ADP
2	>0	high	~0	slow	substrate
3	>0	high	high	fast	respiratory chain
4	>0	low	high	slow	ADP
5	0	high	high	0	oxygen

858 **2.6.1. State 1** is obtained after addition of isolated mitochondria to air-saturated
 859 isoosmotic/isotonic respiration medium containing P_i, but no fuel substrates and no adenylates.
 860

861 **2.6.2. State 2** is induced by addition of a 'high' concentration of ADP (typically 100 to 300 μM),
 862 which stimulates respiration transiently on the basis of endogenous fuel substrates and phosphorylates
 863 only a small portion of the added ADP. State 2 is then obtained at a low respiratory activity limited by
 864 exhausted endogenous fuel substrate availability (**Table 3**). If addition of specific inhibitors of
 865 respiratory complexes such as rotenone does not cause a further decline of O₂ flux, State 2 is equivalent
 866 to the ROX state (See below.). If inhibition is observed, undefined endogenous fuel substrates are a
 867 confounding factor of pathway control, contributing to the effect of subsequently externally added
 868 substrates and inhibitors. In contrast to the original protocol, an alternative sequence of titration steps is
 869 frequently applied, in which the alternative 'State 2' has an entirely different meaning when this second
 870 state is induced by addition of fuel substrate without ADP or ATP (LEAK-state; in contrast to State 2
 871 defined in **Table 1** as a ROX state). Some researchers have called this condition as 'pseudostate 4'
 872 because it has no significant concentrations of adenine nucleotides and hence it is not a near-
 873 physiological condition, although it should be used for calculating the net OXPHOS-capacity, *P-L*.
 874

875 **2.6.3. State 3** is the state stimulated by addition of fuel substrates while the ADP concentration
 876 is still high (**Table 3**) and supports coupled energy transformation through oxidative phosphorylation.
 877 'High ADP' is a concentration of ADP specifically selected to allow the measurement of State 3 to State
 878 4 transitions of isolated mitochondria in a closed respirometric chamber. Repeated ADP titration re-
 879 establishes State 3 at 'high ADP'. Starting at O₂ concentrations near air-saturation (193 or 238 μM O₂
 880 at 37 °C or 25 °C and sea level at 1 atm or 101.32 kPa, and an oxygen solubility of respiration medium
 at 0.92 times that of pure water; Forstner and Gnaiger 1983), the total ADP concentration added must

881 be low enough (typically 100 to 300 μM) to allow phosphorylation to ATP at a coupled O_2 flux that
 882 does not lead to O_2 depletion during the transition to State 4. In contrast, kinetically-saturating ADP
 883 concentrations usually are 10-fold higher than 'high ADP', e.g., 2.5 mM in isolated mitochondria. The
 884 abbreviation State 3u is occasionally used in bioenergetics, to indicate the state of respiration after
 885 titration of an uncoupler, without sufficient emphasis on the fundamental difference between OXPHOS-
 886 capacity (*well-coupled* with an endogenous uncoupled component) and ET-capacity (*noncoupled*).

887 **2.6.4. State 4** is a LEAK-state that is obtained only if the mitochondrial preparation is intact and
 888 well-coupled. Depletion of ADP by phosphorylation to ATP causes a decline of O_2 flux in the transition
 889 from State 3 to State 4. Under the conditions of State 4, a maximum protonmotive force and high
 890 ATP/ADP ratio are maintained. The gradual decline of Y_{P}/O_2 towards diminishing [ADP] at State 4 must
 891 be taken into account for calculation of P/O_2 ratios (Gnaiger 2001). State 4 respiration, L_T (**Table 1**),
 892 reflects intrinsic proton leak and ATP hydrolysis activity. O_2 flux in State 4 is an overestimation of
 893 LEAK-respiration if the contaminating ATP hydrolysis activity recycles some ATP to ADP, J_{P_s} , which
 894 stimulates respiration coupled to phosphorylation, $J_{\text{P}_s} > 0$. Some degree of mechanical disruption and
 895 loss of mitochondrial integrity allows the exposed mitochondrial F-ATPases to hydrolyze the ATP
 896 synthesized by the fraction of coupled mitochondria. This can be tested by inhibition of the
 897 phosphorylation-pathway using oligomycin, ensuring that $J_{\text{P}_s} = 0$ (State 4o). On the other hand, the State
 898 4 respiration reached after exhaustion of added ADP is a more physiological condition, i.e., presence of
 899 ATP, ADP and even AMP. Sequential ADP titrations re-establish State 3, followed by State 3 to State
 900 4 transitions while sufficient O_2 is available. Anoxia may be reached, however, before exhaustion of
 901 ADP (State 5).

902 **2.6.5. State 5** 'may be obtained by antimycin A treatment or by anaerobiosis' (Chance and
 903 Williams, 1955) 'These definitions give State 5 two different meanings of ROX or anoxia, respectively.
 904 Anoxia is obtained after exhaustion of O_2 in a closed respirometric chamber. Diffusion of O_2 from the
 905 surroundings into the aqueous solution may be a confounding factor preventing complete anoxia
 906 (Gnaiger 2001).

907 In **Table 3**, only States 3 and 4 are coupling control states, with the restriction that rates in State
 908 3 may be limited kinetically by non-saturating ADP concentrations.

910 2.7. Control and regulation

911 The terms metabolic *control* and *regulation* are frequently used synonymously, but are
 912 distinguished in metabolic control analysis: "We could understand the regulation as the mechanism that
 913 occurs when a system maintains some variable constant over time, in spite of fluctuations in external
 914 conditions (homeostasis of the internal state). On the other hand, metabolic control is the power to
 915 change the state of the metabolism in response to an external signal" (Fell 1997). Respiratory control
 916 may be induced by experimental control signals that exert an influence on: (1) ATP demand and ADP
 917 phosphorylation-rate; (2) fuel substrate composition, pathway competition; (3) available amounts of
 918 substrates and O_2 , e.g., starvation and hypoxia; (4) the protonmotive force, redox states, flux-force
 919 relationships, coupling and efficiency; (5) Ca^{2+} and other ions including H^+ ; (6) inhibitors, e.g., nitric
 920 oxide or intermediary metabolites such as oxaloacetate; (7) signalling pathways and regulatory proteins,
 921 e.g., insulin resistance, transcription factor hypoxia inducible factor 1.

922 Mechanisms of respiratory control and regulation include adjustments of: (1) enzyme activities
 923 by allosteric mechanisms and phosphorylation; (2) enzyme content, concentrations of cofactors and
 924 conserved moieties such as adenylates, nicotinamide adenine dinucleotide [NAD^+/NADH], coenzyme
 925 Q, cytochrome *c*; (3) metabolic channeling by supercomplexes; and (4) mitochondrial density (enzyme
 926 concentrations and membrane area) and morphology (cristae folding, fission and fusion). Mitochondria
 927 are targeted directly by hormones, e.g., progesterone and glucocorticoids, which affect their energy
 928 metabolism (Lee *et al.* 2013; Gerö and Szabo 2016; Price and Dai 2016; Moreno *et al.* 2017; Singh *et al.*
 929 2018). Evolutionary or acquired differences in the genetic and epigenetic basis of mitochondrial
 930 function (or dysfunction) between individuals; age; biological sex, and hormone concentrations; life
 931 style including exercise and nutrition; and environmental issues including thermal, atmospheric, toxic
 932 and pharmacological factors, exert an influence on all control mechanisms listed above. For reviews,
 933 see Brown 1992; Gnaiger 1993a, 2009; 2014; Paradies *et al.* 2014; Morrow *et al.* 2017.

934 Lack of control by a metabolic pathway, e.g., phosphorylation-pathway, means that there will
 935 be no response to a variable activating it, e.g., [ADP]. The reverse, however, is not true as the absence
 936

937 of a response to [ADP] does not exclude the phosphorylation-pathway from having some degree of
 938 control. The degree of control of a component of the OXPHOS-pathway on an output variable, such as
 939 O₂ flux, will in general be different from the degree of control on other outputs, such as phosphorylation-
 940 flux or proton leak flux. Therefore, it is necessary to be specific as to which input and output are under
 941 consideration (Fell 1997).

942 Respiratory control refers to the ability of mitochondria to adjust O₂ flux in response to external
 943 control signals by engaging various mechanisms of control and regulation. Respiratory control is
 944 monitored in a mitochondrial preparation under conditions defined as respiratory states, preferentially
 945 under near-physiological conditions of temperature, pH, and medium ionic composition, to generate
 946 data of higher biological relevance. When phosphorylation of ADP to ATP is stimulated or depressed,
 947 an increase or decrease is observed in electron transfer measured as O₂ flux in respiratory coupling states
 948 of intact mitochondria ('controlled states' in the classical terminology of bioenergetics). Alternatively,
 949 coupling of electron transfer with phosphorylation is diminished by uncouplers. The corresponding
 950 coupling control state is characterized by a high respiratory rate without control by P» (noncoupled or
 951 'uncontrolled state').

952
 953

954 3. What is a rate?

955

956 The term *rate* is not adequately defined to be useful for reporting data. Normalization of 'rates'
 957 leads to a diversity of formats. Application of common and defined units is required for direct transfer
 958 of reported results into a database. The second [s] is the SI unit for the base quantity *time*. It is also the
 959 standard time-unit used in solution chemical kinetics.

960 The inconsistency of the meanings of rate becomes apparent when considering Galileo Galilei's
 961 famous principle, that 'bodies of different weight all fall at the same rate (have a constant acceleration)'
 962 (Coopersmith 2010). A rate may be an extensive quantity, which is a *flow*, *I*, when expressed per object
 963 (per number of cells or organisms) or per chamber (per system). 'System' is defined as the open or
 964 closed chamber of the measuring device. A rate is a *flux*, *J*, when expressed as a size-specific quantity
 965 (Figure 6A; Box 2).

966 • **Extensive quantities:** An extensive quantity increases proportionally with system size. For
 967 example, mass and volume are extensive quantities. Flow is an extensive quantity. The
 968 magnitude of an extensive quantity is completely additive for non-interacting subsystems.
 969 The magnitude of these quantities depends on the extent or size of the system (Cohen *et al.*
 970 2008).

971 • **Size-specific quantities:** 'The adjective *specific* before the name of an extensive quantity is
 972 often used to mean *divided by mass*' (Cohen *et al.* 2008). In this system-paradigm, mass-
 973 specific flux is flow divided by mass of the system (the total mass of everything within the
 974 measuring chamber or reactor). Rates are frequently expressed as volume-specific flux. A
 975 mass-specific or volume-specific quantity is independent of the extent of non-interacting
 976 homogenous subsystems. Tissue-specific quantities (related to the *sample* in contrast to the
 977 *system*) are of fundamental interest in the field of comparative mitochondrial physiology,
 978 where *specific* refers to the *type of the sample* rather than *mass of the system*. The term
 979 *specific*, therefore, must be clarified; *sample-specific*, *e.g.*, muscle mass-specific
 980 normalization, is distinguished from *system-specific* quantities (mass or volume; Figure 6).

981 • **Intensive quantities:** In contrast to size-specific properties, forces are intensive quantities
 982 defined as the change of an extensive quantity per advancement of an energy transformation
 983 (Gnaiger 1993b).

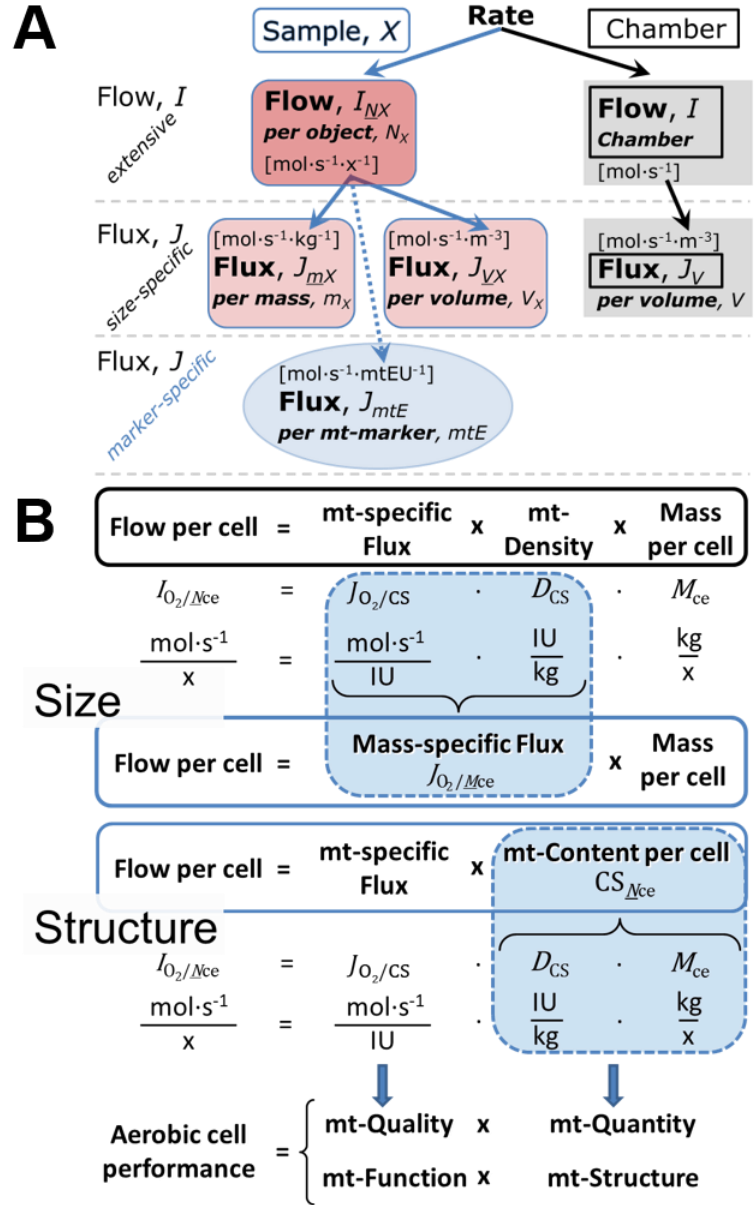
984 • **Formats:** The quantity of a sample *X* can be expressed in different formats. n_X , N_X , and m_X
 985 are the molar amount, number, and mass of *X*, respectively. When different formats are
 986 indicated in symbols of derived quantities, the format (\underline{n} , \underline{N} , \underline{m}) is shown as a subscript
 987 (*underlined italic*), as in $I_{O_2/\underline{N}X}$ and $J_{O_2/\underline{m}X}$. Oxygen flow and flux are expressed in the molar
 988 format, n_{O_2} [mol], but in the volume format, V_{O_2} [m³] in ergometry. For mass-specific flux
 989 these formats can be distinguished as $J_{\underline{n}O_2/\underline{m}X}$ and $J_{\underline{V}O_2/\underline{m}X}$, respectively. Further examples are
 990 given in Figure 6 and Table 4.

991

992 **Figure 6. Flow and flux, and**
 993 **normalization in structure-**
 994 **function analysis**

995 (A) When expressing metabolic
 996 ‘rate’ measured in a chamber, a
 997 fundamental distinction is made
 998 between relating the rate to the
 999 experimental sample (left) or
 1000 chamber (right). The different
 1001 meanings of rate need to be
 1002 specified by the chosen
 1003 normalization. Left: Results are
 1004 expressed as mass-specific flux, J_{mX} ,
 1005 per mg protein, dry or wet mass.
 1006 Cell volume, V_{ce} , may be used for
 1007 normalization (volume-specific
 1008 flux, J_{Vce}). Right: Flow per chamber,
 1009 I , or flux per chamber volume, J_V ,
 1010 are merely reported for
 1011 methodological reasons.

1012 (B) O_2 flow per cell, $I_{O_2/Nce}$, is the
 1013 product of mitochondria-specific
 1014 flux, mt-density and mass per cell.
 1015 Unstructured analysis: performance
 1016 is the product of mass-specific flux,
 1017 $J_{O_2/MX}$ [$\text{mol}\cdot\text{s}^{-1}\cdot\text{kg}^{-1}$], and size
 1018 (mass per cell). Structured analysis:
 1019 performance is the product of
 1020 mitochondrial function (mt-specific
 1021 flux) and structure (mt-content).
 1022 Modified from Gnaiger (2014). For
 1023 further details see **Table 4**.



1029 **Box 2: Metabolic flows and fluxes: vectoral, vectorial, and scalar**

1030
 1031 In a generalization of electrical terms, flow as an extensive quantity (I ; per system) is
 1032 distinguished from flux as a size-specific quantity (J ; per system size). *Flows*, I_{tr} , are defined for all
 1033 transformations as extensive quantities. Electric charge per unit time is electric flow or current, $I_{el} =$
 1034 $dQ_{el} \cdot dt^{-1}$ [$A \equiv C \cdot s^{-1}$]. When dividing I_{el} by size of the system (cross-sectional area of a ‘wire’), we obtain
 1035 flux as a size-specific quantity, which is the current density (surface-density of flow) perpendicular to
 1036 the direction of flux, $J_{el} = I_{el} \cdot A^{-1}$ [$A \cdot m^{-2}$] (Cohen et al. 2008). Fluxes with *spatial* geometric direction and
 1037 magnitude are *vectors*. Vector and scalar *fluxes* are related to flows as $J_{tr} = I_{tr} \cdot A^{-1}$ [$\text{mol}\cdot\text{s}^{-1}\cdot\text{m}^{-2}$] and $J_{tr} =$
 1038 $I_{tr} \cdot V^{-1}$ [$\text{mol}\cdot\text{s}^{-1}\cdot\text{m}^{-3}$], expressing flux as an area-specific vector or volume-specific vectorial or scalar
 1039 quantity, respectively (Gnaiger 1993b). We use the metre–kilogram–second–ampere (MKSA)
 1040 international system of units (SI) for general cases ([m], [kg], [s] and [A]), with decimal SI prefixes for
 1041 specific applications (**Table 4**).

1042 We suggest defining: (1) *vectoral* fluxes, which are translocations as functions of *gradients* with
 1043 direction in geometric space in continuous systems; (2) *vectorial* fluxes, which describe translocations
 1044 in discontinuous systems and are restricted to information on *compartmental differences*
 1045 (transmembrane proton flux); and (3) *scalar* fluxes, which are transformations in a *homogenous* system
 1046 (catabolic O_2 flux, J_{kO_2}).

1047 **4. Normalization of rate per sample**

1048

1049

1050

1051

1052

1053

1054

The challenges of measuring mitochondrial respiratory flux are matched by those of normalization. Normalization (**Table 4**) is guided by physicochemical principles, methodological considerations, and conceptual strategies (**Figure 6**).

Table 4. Sample concentrations and normalization of flux.

Expression	Symbol	Definition	Unit	Notes
Sample				
identity of sample	X	object: cell, tissue, animal, patient		
number of sample entities X	N_X	number of objects	x	1
mass of sample X	m_X		kg	2
mass of object X	M_X	$M_X = m_X \cdot N_X^{-1}$	$\text{kg} \cdot \text{x}^{-1}$	2
Mitochondria				
mitochondria	mt	$X = \text{mt}$		
amount of mt-elementary components	mtE	quantity of mt-marker	mtEU	
Concentrations				
object number concentration	C_{NX}	$C_{NX} = N_X \cdot V^{-1}$	$\text{x} \cdot \text{m}^{-3}$	3
sample mass concentration	C_{mX}	$C_{mX} = m_X \cdot V^{-1}$	$\text{kg} \cdot \text{m}^{-3}$	
mitochondrial concentration	C_{mtE}	$C_{mtE} = mtE \cdot V^{-1}$	$\text{mtEU} \cdot \text{m}^{-3}$	4
specific mitochondrial density	D_{mtE}	$D_{mtE} = mtE \cdot m_X^{-1}$	$\text{mtEU} \cdot \text{kg}^{-1}$	5
mitochondrial content, mtE per object X	mtE_{NX}	$mtE_{NX} = mtE \cdot N_X^{-1}$	$\text{mtEU} \cdot \text{x}^{-1}$	6
O₂ flow and flux				
flow, system	I_{O_2}	internal flow	$\text{mol} \cdot \text{s}^{-1}$	7
volume-specific flux	J_{V,O_2}	$J_{V,O_2} = I_{O_2} \cdot V^{-1}$	$\text{mol} \cdot \text{s}^{-1} \cdot \text{m}^{-3}$	8
flow per object X	$I_{O_2/NX}$	$I_{O_2/NX} = J_{V,O_2} \cdot C_{NX}^{-1}$	$\text{mol} \cdot \text{s}^{-1} \cdot \text{x}^{-1}$	9
mass-specific flux	$J_{O_2/mX}$	$J_{O_2/mX} = J_{V,O_2} \cdot C_{mX}^{-1}$	$\text{mol} \cdot \text{s}^{-1} \cdot \text{kg}^{-1}$	10
mt-marker-specific flux	$J_{O_2/mtE}$	$J_{O_2/mtE} = J_{V,O_2} \cdot C_{mtE}^{-1}$	$\text{mol} \cdot \text{s}^{-1} \cdot \text{mtEU}^{-1}$	11

1055

1056

1057

1058

1059

1060

1061

1062

1063

1064

1065

1066

1067

1068

1069

1070

1071

1072

1 The unit x for a number is not used by IUPAC. To avoid confusion, the units $[\text{kg} \cdot \text{x}^{-1}]$ and $[\text{kg}]$ distinguish the mass per object from the mass of a sample that may contain any number of objects. Similarly, the units for flow per system *versus* flow per object are $[\text{mol} \cdot \text{s}^{-1}]$ (Note 8) and $[\text{mol} \cdot \text{s}^{-1} \cdot \text{x}^{-1}]$ (Note 10).

2 Units are given in the MKSA system (**Box 2**). The SI prefix k is used for the SI base unit of mass (kg = 1,000 g). In praxis, various SI prefixes are used for convenience, to make numbers easily readable, e.g., 1 mg tissue, cell or mitochondrial mass instead of 0.000001 kg.

3 In case of cells (sample $X = \text{cells}$), the object number concentration is $C_{N_{ce}} = N_{ce} \cdot V^{-1}$, and volume may be expressed in $[\text{dm}^3 \equiv \text{L}]$ or $[\text{cm}^3 = \text{mL}]$. See **Table 5** for different object types.

4 mt-concentration is an experimental variable, dependent on sample concentration: (1) $C_{mtE} = mtE \cdot V^{-1}$; (2) $C_{mtE} = mtE_{NX} \cdot C_{NX}$; (3) $C_{mtE} = C_{mX} \cdot D_{mtE}$.

5 If the amount of mitochondria, mtE , is expressed as mitochondrial mass, then D_{mtE} is the mass fraction of mitochondria in the sample. If mtE is expressed as mitochondrial volume, V_{mt} , and the mass of sample, m_X , is replaced by volume of sample, V_X , then D_{mtE} is the volume fraction of mitochondria in the sample.

6 $mtE_{NX} = mtE \cdot N_X^{-1} = C_{mtE} \cdot C_{NX}^{-1}$.

7 O₂ can be replaced by other chemicals to study different reactions, e.g., ATP, H₂O₂, or vesicular compartmental translocations, e.g., Ca²⁺.

- 1073 8 I_{O_2} and V are defined per instrument chamber as a system of constant volume (and constant
 1074 temperature), which may be closed or open. I_{O_2} is abbreviated for I_{rO_2} , *i.e.*, the metabolic or internal
 1075 O_2 flow of the chemical reaction r in which O_2 is consumed, hence the negative stoichiometric
 1076 number, $\nu_{O_2} = -1$. $I_{rO_2} = d_r n_{O_2} / dt \cdot \nu_{O_2}^{-1}$. If r includes all chemical reactions in which O_2 participates, then
 1077 $d_r n_{O_2} = dn_{O_2} - d_e n_{O_2}$, where dn_{O_2} is the change in the amount of O_2 in the instrument chamber and $d_e n_{O_2}$
 1078 is the amount of O_2 added externally to the system. At steady state, by definition $dn_{O_2} = 0$, hence $d_r n_{O_2}$
 1079 $= -d_e n_{O_2}$. Note that in this context ‘external’, e , refers to the system, whereas in Figure 1 ‘external’,
 1080 ext , refers to the organism.
 1081 9 J_{V,O_2} is an experimental variable, expressed per volume of the instrument chamber.
 1082 10 $I_{O_2/NX}$ is a physiological variable, depending on the size of entity X .
 1083 11 There are many ways to normalize for a mitochondrial marker, that are used in different experimental
 1084 approaches: (1) $J_{O_2/mtE} = J_{V,O_2} \cdot C_{mtE}^{-1}$; (2) $J_{O_2/mtE} = J_{V,O_2} \cdot C_{mX}^{-1} \cdot D_{mtE}^{-1} = J_{O_2/mX} \cdot D_{mtE}^{-1}$; (3) $J_{O_2/mtE} =$
 1085 $J_{V,O_2} \cdot C_{NX}^{-1} \cdot mtE_{NX}^{-1} = I_{O_2/NX} \cdot mtE_{NX}^{-1}$; (4) $J_{O_2/mtE} = I_{O_2} \cdot mtE^{-1}$. The mt-elementary unit [mtEU] varies depending
 1086 on the mt-marker.
 1087
 1088
 1089

Table 5. Sample types, X, abbreviations, and quantification.

Identity of sample	X	N_X	Mass ^a	Volume	mt-Marker
mitochondrial preparation		[x]	[kg]	[m ³]	[mtEU]
isolated mitochondria	imt		m_{mt}	V_{mt}	mtE
tissue homogenate	thom		m_{thom}		mtE_{thom}
permeabilized tissue	pti		m_{pti}		mtE_{pti}
permeabilized fibre	pfi		m_{pfi}		mtE_{pfi}
permeabilized cell	pce	N_{pce}	M_{pce}	V_{pce}	mtE_{pce}
cells ^b	ce	N_{ce}	M_{ce}	V_{ce}	mtE_{ce}
intact cell, viable cell	vce	N_{vce}	M_{vce}	V_{vce}	
dead cell	dce	N_{dce}	M_{dce}	V_{dce}	
organism	org	N_{org}	M_{org}	V_{org}	

^a Instead of mass, the wet weight or dry weight is frequently stated, W_w or W_d . m_X is mass of the sample [kg], M_X is mass of the object [kg·x⁻¹] (Table 4).

^b Total cell count, $N_{ce} = N_{vce} + N_{dce}$

4.1. Flow: per object

4.1.1. Number concentration, C_{NX} : Normalization per sample concentration is routinely required to report respiratory data. C_{NX} is the experimental number concentration of sample X . In the case of animals, *e.g.*, nematodes, $C_{NX} = N_X \cdot V^{-1}$ [x·L⁻¹], where N_X is the number of organisms in the chamber. Similarly, the number of cells per chamber volume is the number concentration of permeabilized or intact cells $C_{Nce} = N_{ce} \cdot V^{-1}$ [x·L⁻¹], where N_{ce} is the number of cells in the chamber (Table 4).

4.1.2. Flow per object, $I_{O_2/NX}$: O_2 flow per cell is calculated from volume-specific O_2 flux, J_{V,O_2} [nmol·s⁻¹·L⁻¹] (per V of the measurement chamber [L]), divided by the number concentration of cells. The total cell count is the sum of viable and dead cells, $N_{ce} = N_{vce} + N_{dce}$ (Table 5). The cell viability index, $VI = N_{vce} \cdot N_{ce}^{-1}$, is the ratio of viable cells (N_{vce} ; before experimental permeabilization) per total cell count. After experimental permeabilization, all cells are permeabilized, $N_{pce} = N_{ce}$. The cell viability index can be used to normalize respiration for the number of cells that have been viable before experimental permeabilization, $I_{O_2/Nvce} = I_{O_2/Nce} \cdot VI^{-1}$, considering that mitochondrial respiratory dysfunction in dead cells should be eliminated as a confounding factor.

The complexity changes when the object is a whole organism studied as an experimental model. The scaling law in respiratory physiology reveals a strong interaction between O_2 flow and individual body mass: *basal* metabolic rate (flow) does not increase linearly with body mass, whereas *maximum* mass-specific O_2 flux, \dot{V}_{O_2max} or \dot{V}_{O_2peak} , is approximately constant across a large range of individual body mass (Weibel and Hoppeler 2005). Individuals, breeds and species, however, deviate substantially from this relationship. \dot{V}_{O_2peak} of human endurance athletes is 60 to 80 mL $O_2 \cdot \text{min}^{-1} \cdot \text{kg}^{-1}$ body mass, converted to $J_{O_2peak/Morg}$ of 45 to 60 nmol·s⁻¹·g⁻¹ (Gnaiger 2014; Table 6).

1116 4.2. Size-specific flux: per sample size

1117
1118 **4.2.1. Sample concentration, C_{mX} :** Considering permeabilized tissue, homogenate or cells as the
1119 sample, X , the sample mass is m_X [mg], which is frequently measured as wet or dry weight, W_w or W_d
1120 [mg], respectively, or as amount of protein, m_{Protein} . The sample concentration is the mass of the
1121 subsample per volume of the measurement chamber, $C_{mX} = m_X \cdot V^{-1}$ [$\text{g} \cdot \text{L}^{-1} = \text{mg} \cdot \text{mL}^{-1}$]. X is the type of
1122 sample—isolated mitochondria, tissue homogenate, permeabilized fibres or cells (**Table 5**).

1123 **4.2.2. Size-specific flux:** Cellular O_2 flow can be compared between cells of identical size. To
1124 take into account changes and differences in cell size, normalization is required to obtain cell size-
1125 specific or mitochondrial marker-specific O_2 flux (Renner *et al.* 2003).

- 1126 • **Mass-specific flux, $J_{\text{O}_2/mX}$ [$\text{mol} \cdot \text{s}^{-1} \cdot \text{kg}^{-1}$]:** Mass-specific flux is obtained by expressing
1127 respiration per mass of sample, m_X [mg]. Flow per cell is divided by mass per cell, $J_{\text{O}_2/mce} =$
1128 $I_{\text{O}_2/Nce} \cdot M_{Nce}^{-1}$. Or chamber volume-specific flux, J_{V,O_2} , is divided by mass concentration of X in
1129 the chamber, $J_{\text{O}_2/mX} = J_{V,\text{O}_2} \cdot C_{mX}^{-1}$.
- 1130 • **Cell volume-specific flux, $J_{\text{O}_2/VX}$ [$\text{mol} \cdot \text{s}^{-1} \cdot \text{m}^{-3}$]:** Sample volume-specific flux is obtained by
1131 expressing respiration per volume of sample. For example, in the case of using cells as sample
1132 will be the volume of cells added to the chamber (**Figure 6**).

1133 If size-specific O_2 flux is constant and independent of sample size, then there is no interaction
1134 between the subsystems. For example, a 1.5 mg and a 3.0 mg muscle sample respire at identical mass-
1135 specific flux. Mass-specific O_2 flux, however, may change with the mass of a tissue sample, cells or
1136 isolated mitochondria in the measuring chamber, in which the nature of the interaction becomes an issue.
1137 Therefore, cell density must be optimized, particularly in experiments carried out in wells, considering
1138 the confluency of the cell monolayer or clumps of cells (Salabei *et al.* 2014).

1139 4.3. Marker-specific flux: per mitochondrial content

1140
1141 Tissues can contain multiple cell populations that may have distinct mitochondrial subtypes.
1142 Mitochondria undergo dynamic fission and fusion cycles, and can exist in multiple stages and sizes that
1143 may be altered by a range of factors. The isolation of mitochondria (often achieved through differential
1144 centrifugation) can therefore yield a subsample of the mitochondrial types present in a tissue, depending
1145 on the isolation protocols utilized, *e.g.*, centrifugation speed. This possible bias should be taken into
1146 account when planning experiments using isolated mitochondria. Different sizes of mitochondria are
1147 enriched at specific centrifugation speeds, which can be used strategically for isolation of mitochondrial
1148 subpopulations.

1149 Part of the mitochondrial content of a tissue is lost during preparation of isolated mitochondria.
1150 The fraction of isolated mitochondria obtained from a tissue sample is expressed as mitochondrial
1151 recovery. At a high mitochondrial recovery, the fraction of isolated mitochondria is more representative
1152 of the total mitochondrial population than in preparations characterized by low recovery. Determination
1153 of the mitochondrial recovery and yield is based on measurement of the concentration of a mitochondrial
1154 marker in the stock of isolated mitochondria, $C_{mtE,\text{stock}}$, and crude tissue homogenate, $C_{mtE,\text{thom}}$, which
1155 simultaneously provides information on the specific mitochondrial density in the sample, D_{mtE} (**Table**
1156 **4**).
1157

1158 When discussing concepts of normalization, it is essential to consider the question posed by the
1159 study. If the study aims at comparing tissue performance—such as the effects of a treatment on a specific
1160 tissue, then normalization for tissue mass or protein content is appropriate. However, if the aim is to
1161 find differences in mitochondrial function independent of mitochondrial density (**Table 4**), then
1162 normalization to a mitochondrial marker is imperative (**Figure 6**). One cannot assume that quantitative
1163 changes in various markers—such as mitochondrial proteins—necessarily occur in parallel with one
1164 another. It should be established that the marker chosen is not selectively altered by the performed
1165 treatment. In conclusion, the normalization must reflect the question under investigation to reach a
1166 satisfying answer. On the other hand, the goal of comparing results across projects and institutions
1167 requires standardization on normalization for entry into a databank.

1168 **4.3.1. Mitochondrial concentration, C_{mtE} , and mitochondrial markers:** Mitochondrial
1169 organelles compose a dynamic cellular reticulum in various states of fusion and fission. Hence, the
1170 definition of an ‘amount’ of mitochondria is often misconceived: mitochondria cannot be counted
1171 reliably as a number of occurring elementary components. Therefore, quantification of the amount of

1172 mitochondria depends on the measurement of chosen mitochondrial markers. “Mitochondria are the
 1173 structural and functional elementary units of cell respiration” (Gnaiger 2014). The quantity of a
 1174 mitochondrial marker can reflect the amount of *mitochondrial elementary components*, mtE , expressed
 1175 in various mitochondrial elementary units [mtEU] specific for each measured mt-marker (**Table 4**).
 1176 However, since mitochondrial quality may change in response to stimuli—particularly in mitochondrial
 1177 dysfunction (Campos *et al.* 2017) and after exercise training (Pesta *et al.* 2011) and during aging (Daum
 1178 *et al.* 2013)—some markers can vary while others are unchanged: (1) Mitochondrial volume and
 1179 membrane area are structural markers, whereas mitochondrial protein mass is commonly used as a
 1180 marker for isolated mitochondria. (2) Molecular and enzymatic mitochondrial markers (amounts or
 1181 activities) can be selected as matrix markers, *e.g.*, citrate synthase activity, mtDNA; mtIM-markers, *e.g.*,
 1182 cytochrome *c* oxidase activity, aa_3 content, cardiolipin, or mtOM-markers, *e.g.*, the voltage-dependent
 1183 anion channel (VDAC), TOM20. (3) Extending the measurement of mitochondrial marker enzyme
 1184 activity to mitochondrial pathway capacity, ET- or OXPHOS-capacity can be considered as an
 1185 integrative functional mitochondrial marker.

1186 Depending on the type of mitochondrial marker, the mitochondrial elementary component, mtE ,
 1187 is expressed in marker-specific units. Mitochondrial concentration in the measurement chamber and the
 1188 tissue of origin are quantified as (1) a quantity for normalization in functional analyses, C_{mtE} , and (2) a
 1189 physiological output that is the result of mitochondrial biogenesis and degradation, D_{mtE} , respectively
 1190 (**Table 4**). It is recommended, therefore, to distinguish *experimental mitochondrial concentration*, C_{mtE}
 1191 $= mtE \cdot V^{-1}$ and *physiological mitochondrial density*, $D_{mtE} = mtE \cdot m_X^{-1}$. Then mitochondrial density is the
 1192 amount of mitochondrial elementary components per mass of tissue, which is a biological variable
 1193 (**Figure 6**). The experimental variable is mitochondrial density multiplied by sample mass concentration
 1194 in the measuring chamber, $C_{mtE} = D_{mtE} \cdot C_{mX}$, or mitochondrial content multiplied by sample number
 1195 concentration, $C_{mtE} = mtE_X \cdot C_{NX}$ (**Table 4**).

1196 **4.3.2. mt-Marker-specific flux, $J_{O_2/mtE}$:** Volume-specific metabolic O_2 flux depends on: (1) the
 1197 sample concentration in the volume of the instrument chamber, C_{mX} , or C_{NX} ; (2) the mitochondrial
 1198 density in the sample, $D_{mtE} = mtE \cdot m_X^{-1}$ or $mtE_X = mtE \cdot N_X^{-1}$; and (3) the specific mitochondrial activity or
 1199 performance per elementary mitochondrial unit, $J_{O_2/mtE} = J_{V,O_2} \cdot C_{mtE}^{-1}$ [$\text{mol} \cdot \text{s}^{-1} \cdot \text{mtEU}^{-1}$] (**Table 4**).
 1200 Obviously, the numerical results for $J_{O_2/mtE}$ vary with the type of mitochondrial marker chosen for
 1201 measurement of mtE and $C_{mtE} = mtE \cdot V^{-1}$ [$\text{mtEU} \cdot \text{m}^{-3}$].

1202 Different methods are involved in the quantification of mitochondrial markers and have different
 1203 strengths. Some problems are common for all mitochondrial markers, mtE : (1) Accuracy of
 1204 measurement is crucial, since even a highly accurate and reproducible measurement of O_2 flux results
 1205 in an inaccurate and noisy expression if normalized by a biased and noisy measurement of a
 1206 mitochondrial marker. This problem is acute in mitochondrial respiration because the denominators used
 1207 (the mitochondrial markers) are often small moieties of which accurate and precise determination is
 1208 difficult. This problem can be avoided when O_2 fluxes measured in substrate-uncoupler-inhibitor
 1209 titration protocols are normalized for flux in a defined respiratory reference state, which is used as an
 1210 *internal* marker and yields flux control ratios, $FCRs$. $FCRs$ are independent of externally measured
 1211 markers and, therefore, are statistically robust, considering the limitations of ratios in general (Jasienski
 1212 and Bazzaz 1999). $FCRs$ indicate qualitative changes of mitochondrial respiratory control, with highest
 1213 quantitative resolution, separating the effect of mitochondrial density or concentration on $J_{O_2/mX}$ and
 1214 $I_{O_2/NX}$ from that of function per elementary mitochondrial marker, $J_{O_2/mtE}$ (Pesta *et al.* 2011; Gnaiger
 1215 2014). (2) If mitochondrial quality does not change and only the amount of mitochondria varies as a
 1216 determinant of mass-specific flux, any marker is equally qualified in principle; then in practice selection
 1217 of the optimum marker depends only on the accuracy and precision of measurement of the mitochondrial
 1218 marker. (3) If mitochondrial flux control ratios change, then there may not be any best mitochondrial
 1219 marker. In general, measurement of multiple mitochondrial markers enables a comparison and
 1220 evaluation of normalization for these mitochondrial markers. Particularly during postnatal development,
 1221 the activity of marker enzymes—such as cytochrome *c* oxidase and citrate synthase—follows different
 1222 time courses (Drahota *et al.* 2004). Evaluation of mitochondrial markers in healthy controls is
 1223 insufficient for providing guidelines for application in the diagnosis of pathological states and specific
 1224 treatments.

1225 In line with the concept of the respiratory control ratio (Chance and Williams 1955a), the most
 1226 readily used normalization is that of flux control ratios and flux control factors (Gnaiger 2014). Selection
 1227 of the state of maximum flux in a protocol as the reference state has the advantages of: (1) internal

1228 normalization; (2) statistically validated linearization of the response in the range of 0 to 1; and (3)
 1229 consideration of maximum flux for integrating a large number of elementary steps in the OXPHOS- or
 1230 ET-pathways. This reduces the risk of selecting a functional marker that is specifically altered by the
 1231 treatment or pathology, yet increases the chance that the highly integrative pathway is disproportionately
 1232 affected, *e.g.*, the OXPHOS- rather than ET-pathway in case of an enzymatic defect in the
 1233 phosphorylation-pathway. In this case, additional information can be obtained by reporting flux control
 1234 ratios based on a reference state that indicates stable tissue-mass specific flux.

1235 Stereological measurement of mitochondrial content via two-dimensional transmission electron
 1236 microscopy is considered as the gold standard in determination of mitochondrial volume fractions in
 1237 cells and tissues (Weibel, Hoppeler, 2005). Accurate determination of three-dimensional volume by
 1238 two-dimensional microscopy, however, is both time consuming and statistically challenging (Larsen *et al.*
 1239 *et al.* 2012). The validity of using mitochondrial marker enzymes (citrate synthase activity, CI to CIV
 1240 amount or activity) for normalization of flux is limited in part by the same factors that apply to flux
 1241 control ratios. Strong correlations between various mitochondrial markers and citrate synthase activity
 1242 (Reichmann *et al.* 1985; Boushel *et al.* 2007; Mogensen *et al.* 2007) are expected in a specific tissue of
 1243 healthy persons and in disease states not specifically targeting citrate synthase. Citrate synthase activity
 1244 is acutely modifiable by exercise (Tonkonogi *et al.* 1997; Leek *et al.* 2001). Evaluation of mitochondrial
 1245 markers related to a selected age and sex cohort cannot be extrapolated to provide recommendations for
 1246 normalization in respirometric diagnosis of disease, in different states of development and ageing,
 1247 different cell types, tissues, and species. mtDNA normalized to nDNA via qPCR is correlated to
 1248 functional mitochondrial markers including OXPHOS- and ET-capacity in some cases (Puntschart *et al.*
 1249 1995; Wang *et al.* 1999; Menshikova *et al.* 2006; Boushel *et al.* 2007; Ehinger *et al.* 2015), but lack of
 1250 such correlations have been reported (Menshikova *et al.* 2005; Schultz and Wiesner 2000; Pesta *et al.*
 1251 2011). Several studies indicate a strong correlation between cardiolipin content and increase in
 1252 mitochondrial function with exercise (Menshikova *et al.* 2005; Menshikova *et al.* 2007; Larsen *et al.*
 1253 2012; Faber *et al.* 2014), but it has not been evaluated as a general mitochondrial biomarker in disease.
 1254 With no single best mitochondrial marker, a good strategy is to quantify several different biomarkers to
 1255 minimize the decorrelating effects caused by diseases, treatments, or other factors. Determination of
 1256 multiple markers, particularly a matrix marker and a marker from the mtIM, allows tracking changes in
 1257 mitochondrial quality defined by their ratio.

1260 5. Normalization of rate per system

1262 5.1. Flow: per chamber

1264 The experimental system (experimental chamber) is part of the measurement instrument,
 1265 separated from the environment as an isolated, closed, open, isothermal or non-isothermal system
 1266 (Table 4). Reporting O₂ flows per respiratory chamber, I_{O_2} [nmol·s⁻¹], restricts the analysis to intra-
 1267 experimental comparison of relative differences.

1269 5.2. Flux: per chamber volume

1271 **5.2.1. System-specific flux, J_{V,O_2} :** We distinguish between (1) the *system* with volume V and mass
 1272 m defined by the system boundaries, and (2) the *sample* or *objects* with volume V_X and mass m_X that are
 1273 enclosed in the experimental chamber (Figure 6). Metabolic O₂ flow per object, I_{O_2/N_X} , is the total O₂
 1274 flow in the system divided by the number of objects, N_X , in the system. I_{O_2/N_X} increases as the mass of
 1275 the object is increased. Sample mass-specific O₂ flux, J_{O_2/m_X} should be independent of the mass of the
 1276 sample studied in the instrument chamber, but system volume-specific O₂ flux, J_{V,O_2} (per volume of the
 1277 instrument chamber), increases in proportion to the mass of the sample in the chamber. Although J_{V,O_2}
 1278 depends on mass-concentration of the sample in the chamber, it should be independent of the chamber
 1279 (system) volume at constant sample mass-concentration. There are practical limitations to increasing the
 1280 mass-concentration of the sample in the chamber, when one is concerned about crowding effects and
 1281 instrumental time resolution.

1282 **5.2.2. Advancement per volume:** When the reactor volume does not change during the reaction,
 1283 which is typical for liquid phase reactions, the volume-specific flux of a chemical reaction r is the time

1284 derivative of the advancement of the reaction per unit volume, $J_{V,rB} = d_{r\zeta_B}/dt \cdot V^{-1}$ [(mol·s⁻¹)·L⁻¹]. The *rate*
 1285 *of concentration change* is dc_B/dt [(mol·L⁻¹)·s⁻¹], where concentration is $c_B = n_B \cdot V^{-1}$. There is a difference
 1286 between (1) J_{V,rO_2} [mol·s⁻¹·L⁻¹] and (2) rate of concentration change [mol·L⁻¹·s⁻¹]. These merge into a
 1287 single expression only in closed systems. In open systems, internal transformations (catabolic flux, O₂
 1288 consumption) are distinguished from external flux (such as O₂ supply). External fluxes of all substances
 1289 are zero in closed systems. In a closed chamber O₂ consumption (internal flux of catabolic reactions k ;
 1290 I_{kO_2} [pmol·s⁻¹]) causes a decline in the amount of O₂ in the system, n_{O_2} [nmol]. Normalization of these
 1291 quantities for the volume of the system, V [L \equiv dm³], yields volume-specific O₂ flux, $J_{V,kO_2} = I_{kO_2}/V$
 1292 [nmol·s⁻¹·L⁻¹], and O₂ concentration, [O₂] or $c_{O_2} = n_{O_2} \cdot V^{-1}$ [μ mol·L⁻¹ = μ M = nmol·mL⁻¹]. Instrumental
 1293 background O₂ flux is due to external flux into a non-ideal closed respirometer, so total volume-specific
 1294 flux has to be corrected for instrumental background O₂ flux—O₂ diffusion into or out of the
 1295 instrumental chamber. J_{V,kO_2} is relevant mainly for methodological reasons and should be compared with
 1296 the accuracy of instrumental resolution of background-corrected flux, *e.g.*, ± 1 nmol·s⁻¹·L⁻¹ (Gnaiger
 1297 2001). ‘Catabolic’ indicates O₂ flux, J_{kO_2} , corrected for: (1) instrumental background O₂ flux; (2)
 1298 chemical background O₂ flux due to autoxidation of chemical components added to the incubation
 1299 medium; and (3) *Rox* for O₂-consuming side reactions unrelated to the catabolic pathway k .

1300
1301

1302 6. Conversion of units

1303

1304 Many different units have been used to report the O₂ consumption rate, OCR (Table 6). SI base
 1305 units provide the common reference to introduce the theoretical principles (Figure 6), and are used with
 1306 appropriately chosen SI prefixes to express numerical data in the most practical format, with an effort
 1307 towards unification within specific areas of application (Table 7). Reporting data in SI units—including
 1308 the mole [mol], coulomb [C], joule [J], and second [s]—should be encouraged, particularly by journals
 1309 that propose the use of SI units.

1310

1311 **Table 6. Conversion of various formats and units used in respirometry and**
 1312 **ergometry.** e^- is the number of electrons or reducing equivalents. z_B is the charge number
 1313 of entity B.
 1314

Format	1 Unit		Multiplication factor	SI-unit	Notes
\underline{n}	ng.atom O·s ⁻¹	(2 e ⁻)	0.5	nmol O ₂ ·s ⁻¹	
\underline{n}	ng.atom O·min ⁻¹	(2 e ⁻)	8.33	pmol O ₂ ·s ⁻¹	
\underline{n}	natom O·min ⁻¹	(2 e ⁻)	8.33	pmol O ₂ ·s ⁻¹	
\underline{n}	nmol O ₂ ·min ⁻¹	(4 e ⁻)	16.67	pmol O ₂ ·s ⁻¹	
\underline{n}	nmol O ₂ ·h ⁻¹	(4 e ⁻)	0.2778	pmol O ₂ ·s ⁻¹	
\underline{V} to \underline{n}	mL O ₂ ·min ⁻¹ at STPD ^a		0.744	μ mol O ₂ ·s ⁻¹	1
\underline{e} to \underline{n}	W = J/s at -470 kJ/mol O ₂		-2.128	μ mol O ₂ ·s ⁻¹	
\underline{e} to \underline{n}	mA = mC·s ⁻¹	($z_{H^+} = 1$)	10.36	nmol H ⁺ ·s ⁻¹	2
\underline{e} to \underline{n}	mA = mC·s ⁻¹	($z_{O_2} = 4$)	2.59	nmol O ₂ ·s ⁻¹	2
\underline{n} to \underline{e}	nmol H ⁺ ·s ⁻¹	($z_{H^+} = 1$)	0.09649	mA	3
\underline{n} to \underline{e}	nmol O ₂ ·s ⁻¹	($z_{O_2} = 4$)	0.38594	mA	3

1315 1 At standard temperature and pressure dry (STPD: 0 °C = 273.15 K and 1 atm = 101.325 kPa =
 1316 760 mmHg), the molar volume of an ideal gas, V_m , and V_{m,O_2} is 22.414 and 22.392 L·mol⁻¹,
 1317 respectively. Rounded to three decimal places, both values yield the conversion factor of 0.744.
 1318 For comparison at normal temperature and pressure dry (NTPD: 20 °C), V_{m,O_2} is 24.038 L·mol⁻¹.
 1319 Note that the SI standard pressure is 100 kPa.

1320 2 The multiplication factor is $10^6/(z_B \cdot F)$.

1321 3 The multiplication factor is $z_B \cdot F/10^6$.

1322

1323

Table 7. Conversion of units with preservation of numerical values.

Name	Frequently used unit	Equivalent unit	Notes
volume-specific flux, J_{V,O_2}	$\text{pmol}\cdot\text{s}^{-1}\cdot\text{mL}^{-1}$	$\text{nmol}\cdot\text{s}^{-1}\cdot\text{L}^{-1}$	1
cell-specific flow, $I_{O_2/\text{cell}}$	$\text{mmol}\cdot\text{s}^{-1}\cdot\text{L}^{-1}$	$\text{mol}\cdot\text{s}^{-1}\cdot\text{m}^{-3}$	
	$\text{pmol}\cdot\text{s}^{-1}\cdot 10^{-6}$ cells	$\text{amol}\cdot\text{s}^{-1}\cdot\text{cell}^{-1}$	2
cell number concentration, C_{Nce}	$\text{pmol}\cdot\text{s}^{-1}\cdot 10^{-9}$ cells	$\text{zmol}\cdot\text{s}^{-1}\cdot\text{cell}^{-1}$	3
	10^6 cells $\cdot\text{mL}^{-1}$	10^9 cells $\cdot\text{L}^{-1}$	
mitochondrial protein concentration, C_{mtE}	0.1 mg $\cdot\text{mL}^{-1}$	0.1 g $\cdot\text{L}^{-1}$	
mass-specific flux, $J_{O_2/m}$	$\text{pmol}\cdot\text{s}^{-1}\cdot\text{mg}^{-1}$	$\text{nmol}\cdot\text{s}^{-1}\cdot\text{g}^{-1}$	4
catabolic power, P_k	$\mu\text{W}\cdot 10^{-6}$ cells	$\text{pW}\cdot\text{cell}^{-1}$	1
volume	1,000 L	m^3 (1,000 kg)	
	L	dm^3 (kg)	
	mL	cm^3 (g)	
	μL	mm^3 (mg)	
	fL	μm^3 (pg)	5
amount of substance concentration	$\text{M} = \text{mol}\cdot\text{L}^{-1}$	$\text{mol}\cdot\text{dm}^{-3}$	

1324 1 pmol: picomole = 10^{-12} mol1325 2 amol: attomole = 10^{-18} mol1326 3 zmol: zeptomole = 10^{-21} mol

1327

1328 Although volume is expressed as m^3 using the SI base unit, the litre [dm^3] is a conventional unit
 1329 of volume for concentration and is used for most solution chemical kinetics. If one multiplies $I_{O_2/Nce}$ by
 1330 C_{Nce} , then the result will not only be the amount of O_2 [mol] consumed per time [s^{-1}] in one litre [L^{-1}],
 1331 but also the change in O_2 concentration per second (for any volume of an ideally closed system). This
 1332 is ideal for kinetic modeling as it blends with chemical rate equations where concentrations are typically
 1333 expressed in $\text{mol}\cdot\text{L}^{-1}$ (Wagner *et al.* 2011). In studies of multinuclear cells—such as differentiated
 1334 skeletal muscle cells—it is easy to determine the number of nuclei but not the total number of cells. A
 1335 generalized concept, therefore, is obtained by substituting cells by nuclei as the sample entity. This does
 1336 not hold, however, for non-nucleated platelets.

1337 For studies of cells, we recommend that respiration be expressed, as far as possible, as: (1) O_2
 1338 flux normalized for a mitochondrial marker, for separation of the effects of mitochondrial quality and
 1339 content on cell respiration (this includes $FCRs$ as a normalization for a functional mitochondrial
 1340 marker); (2) O_2 flux in units of cell volume or mass, for comparison of respiration of cells with different
 1341 cell size (Renner *et al.* 2003) and with studies on tissue preparations, and (3) O_2 flow in units of attomole
 1342 (10^{-18} mol) of O_2 consumed per second by each cell [$\text{amol}\cdot\text{s}^{-1}\cdot\text{cell}^{-1}$], numerically equivalent to
 1343 [$\text{pmol}\cdot\text{s}^{-1}\cdot 10^{-6}$ cells]. This convention allows information to be easily used when designing experiments
 1344 in which O_2 flow must be considered. For example, to estimate the volume-specific O_2 flux in an
 1345 instrument chamber that would be expected at a particular cell number concentration, one simply needs
 1346 to multiply the flow per cell by the number of cells per volume of interest. This provides the amount of
 1347 O_2 [mol] consumed per time [s^{-1}] per unit volume [L^{-1}]. At an O_2 flow of 100 $\text{amol}\cdot\text{s}^{-1}\cdot\text{cell}^{-1}$ and a cell
 1348 density of 10^9 cells $\cdot\text{L}^{-1}$ (10^6 cells $\cdot\text{mL}^{-1}$), the volume-specific O_2 flux is 100 $\text{nmol}\cdot\text{s}^{-1}\cdot\text{L}^{-1}$ (100
 1349 $\text{pmol}\cdot\text{s}^{-1}\cdot\text{mL}^{-1}$).

1350 ET-capacity in human cell types including HEK 293, primary HUVEC, and fibroblasts ranges
 1351 from 50 to 180 $\text{amol}\cdot\text{s}^{-1}\cdot\text{cell}^{-1}$, measured in intact cells in the noncoupled state (see Gnaiger 2014). At
 1352 100 $\text{amol}\cdot\text{s}^{-1}\cdot\text{cell}^{-1}$ corrected for Rox , the current across the mt-membranes, I_{H^+e} , approximates 193
 1353 $\text{pA}\cdot\text{cell}^{-1}$ or 0.2 nA per cell. See Rich (2003) for an extension of quantitative bioenergetics from the
 1354 molecular to the human scale, with a transmembrane proton flux equivalent to 520 A in an adult at a
 1355 catabolic power of -110 W. Modelling approaches illustrate the link between protonmotive force and
 1356 currents (Willis *et al.* 2016).

1357 We consider isolated mitochondria as powerhouses and proton pumps as molecular machines to
 1358 relate experimental results to energy metabolism of the intact cell. The cellular P_{\gg}/O_2 based on oxidation

of glycogen is increased by the glycolytic (fermentative) substrate-level phosphorylation of 3 P_»/Glyc or 0.5 mol P_» for each mol O₂ consumed in the complete oxidation of a mol glycosyl unit (Glyc). Adding 0.5 to the mitochondrial P_»/O₂ ratio of 5.4 yields a bioenergetic cell physiological P_»/O₂ ratio close to 6. Two NADH equivalents are formed during glycolysis and transported from the cytosol into the mitochondrial matrix, either by the malate-aspartate shuttle or by the glycerophosphate shuttle (**Figure 2A**) resulting in different theoretical yields of ATP generated by mitochondria, the energetic cost of which potentially must be taken into account. Considering also substrate-level phosphorylation in the TCA cycle, this high P_»/O₂ ratio not only reflects proton translocation and OXPHOS studied in isolation, but integrates mitochondrial physiology with energy transformation in the living cell (Gnaiger 1993a).

7. Conclusions

Catabolic cell respiration is the process of exergonic and exothermic energy transformation in which scalar redox reactions are coupled to vectorial ion translocation across a semipermeable membrane, which separates the small volume of a bacterial cell or mitochondrion from the larger volume of its surroundings. The electrochemical exergy can be partially conserved in the phosphorylation of ADP to ATP or in ion pumping, or dissipated in an electrochemical short-circuit. Respiration is thus clearly distinguished from fermentation as the counterparts of cellular core energy metabolism. An O₂ flux balance scheme illustrates the relationships and general definitions (**Figures 1 and 2**).

Box 3: Recommendations for studies with mitochondrial preparations

- Normalization of respiratory rates should be provided as far as possible:
 1. *Biophysical normalization*: on a per cell basis as O₂ flow; this may not be possible when dealing with coenocytic organisms, *e.g.*, filamentous fungi, or tissues without cross-walls separating individual cells, *e.g.*, muscle fibers.
 2. *Cellular normalization*: per g protein; per cell- or tissue-mass as mass-specific O₂ flux; per cell volume as cell volume-specific flux.
 3. *Mitochondrial normalization*: per mitochondrial marker as mt-specific flux.
- With information on cell size and the use of multiple normalizations, maximum potential information is available (Renner *et al.* 2003; Wagner *et al.* 2011; Gnaiger 2014). Reporting flow in a respiratory chamber [nmol·s⁻¹] is discouraged, since it restricts the analysis to intra-experimental comparison of relative (qualitative) differences.
- Catabolic mitochondrial respiration is distinguished from residual O₂ consumption. Fluxes in mitochondrial coupling states should be, as far as possible, corrected for residual O₂ consumption.
- Different mechanisms of uncoupling should be distinguished by defined terms. The tightness of coupling relates to these uncoupling mechanisms, whereas the coupling stoichiometry varies as a function the substrate type involved in ET-pathways with either three or two redox proton pumps operating in series. Separation of tightness of coupling from the pathway-dependent coupling stoichiometry is possible only when the substrate type undergoing oxidation remains the same for respiration in LEAK-, OXPHOS-, and ET-states. In studies of the tightness of coupling, therefore, simple substrate-inhibitor combinations should be applied to exclude a shift in substrate competition that may occur when providing physiological substrate cocktails.
- In studies of isolated mitochondria, the mitochondrial recovery and yield should be reported. Experimental criteria such as transmission electron microscopy for evaluation of purity versus integrity should be considered. Mitochondrial markers—such as citrate synthase activity as an enzymatic matrix marker—provide a link to the tissue of origin on the basis of calculating the mitochondrial recovery, *i.e.*, the fraction of mitochondrial marker obtained from a unit mass of tissue. Total mitochondrial protein is frequently applied as a mitochondrial marker, which is restricted to isolated mitochondria.
- In studies of permeabilized cells, the viability of the cell culture or cell suspension of origin should be reported. Normalization should be evaluated for total cell count or viable cell count.
- Terms and symbols are summarized in **Table 8**. Their use will facilitate transdisciplinary communication and support further development of a consistent theory of bioenergetics and mitochondrial physiology. Technical terms related to and defined with normal words can be used as

1415 index terms in databases, support the creation of ontologies towards semantic information processing
 1416 (MitoPedia), and help in communicating analytical findings as impactful data-driven stories.
 1417 ‘Making data available without making it understandable may be worse than not making it available
 1418 at all’ (National Academies of Sciences, Engineering, and Medicine 2018). Success will depend on
 1419 taking further steps: (1) exhaustive text-mining considering Omics data and functional data; (2)
 1420 network analysis of Omics data with bioinformatics tools; (3) cross-validation with distinct
 1421 bioinformatics approaches; (4) correlation with functional data; (5) guidelines for biological
 1422 validation of network data. This is a call to carefully contribute to FAIR principles (Findable,
 1423 Accessible, Interoperable, Reusable) for the sharing of scientific data.

1425
1426
1427 **Table 8. Terms, symbols, and units.**
1428
1429

1430 1431	Term	Symbol	Unit	Links and comments
1432	1433 alternative quinol oxidase	AOX		Figure 2B
1434	adenosine monophosphate	AMP		2 ADP ↔ ATP+AMP
1435	adenosine diphosphate	ADP		Table 1; Figures 1, 2 and 5
1436	adenosine triphosphate	ATP		Figures 2 and 5
1437	adenylates	AMP, ADP, ATP		Section 2.5.1
1438	amount of substance B	n_B	[mol]	
1439	ATP yield per O ₂	$Y_{P\gg/O_2}$		P ₂ /O ₂ ratio measured in any respiratory state
1440				
1441	catabolic reaction	k		Figures 1 and 3
1442	catabolic respiration	J_{kO_2}	<i>varies</i>	Figures 1 and 3
1443	cell respiration	J_{rO_2}	<i>varies</i>	Figure 1
1444	cell viability index	VI		$VI = N_{vce} \cdot N_{ce}^{-1} = 1 - N_{dce} \cdot N_{ce}^{-1}$
1445	charge number of entity B	z_B		Table 6; $z_{O_2} = 4$
1446	Complexes I to IV	CI to CIV		respiratory ET Complexes; Figure 2B
1447				
1448	concentration of substance B	$c_B = n_B \cdot V^{-1}$; [B]	[mol·m ⁻³]	Box 2
1449	coupling control state	CCS		Section 2.4.1
1450	dead cell number	N_{dce}	[x]	non-viable cells, loss of plasma membrane barrier function; Table 5
1451				
1452	electric format	\underline{e}	[C]	Table 6
1453	electron transfer system	ETS		state; Figures 2B and 4
1454	ET state	ET		Table 1; Figures 2B and 4; State 3u
1455	ET-capacity	E	<i>varies</i>	Table 1; Figure 4
1456	flow, for substance B	I_B	[mol·s ⁻¹]	system-related extensive quantity; Figure 6
1457				
1458	flux, for substance B	J_B	<i>varies</i>	size-specific quantity; Figure 6
1459	inorganic phosphate	P _i		Figure 2C
1460	inorganic phosphate carrier	PiC		Figure 2C
1461	intact cell number,			
1462	viable cell number	N_{vce}	[x]	viable cells, intact plasma membrane barrier function; Table 5
1463				
1464	LEAK state	LEAK		state; Table 1; Figure 4; compare State 4
1465				
1466	LEAK-respiration	L	<i>varies</i>	Table 1; Figure 4
1467	mass format	\underline{m}	[kg]	Table 4; Figure 6
1468	mass of sample X	m_X	[kg]	Table 4
1469	mass, dry mass	m_d	[kg]	mass of sample X; Figure 6 (frequently called dry weight)
1470				
1471	mass, wet mass	m_w	[kg]	mass of sample X; Figure 6 (frequently called wet weight)
1472				

1473	mass of object X	$M_X = m_X \cdot N_X^{-1}$	$[\text{kg} \cdot \text{x}^{-1}]$	mass of entity X ; Table 4
1474	MITOCARTA			https://www.broadinstitute.org/scientific-community/science/programs/metabolic-disease-program/publications/mitocarta/mitocarta-in-0
1475				
1476				
1477				
1478				
1479	MitoPedia			http://www.bioblast.at/index.php/MitoPedia
1480	mitochondria or mitochondrial	mt		Box 1
1481	mitochondrial DNA	mtDNA		Box 1
1482	mitochondrial concentration	$C_{mtE} = mtE \cdot V^{-1}$	$[\text{mtEU} \cdot \text{m}^{-3}]$	Table 4
1483	mitochondrial content	mtE_X	$[\text{mtEU} \cdot \text{x}^{-1}]$	$mtE_X = mtE \cdot N_X^{-1}$; Table 4
1484	mitochondrial			
1485	elementary component	mtE	$[\text{mtEU}]$	quantity of mt-marker; Table 4
1486	mitochondrial elementary unit	mtEU	<i>varies</i>	specific units for mt-marker; Table 4
1487	mitochondrial inner membrane	mtIM		MIM is widely used; the first M is replaced by mt; Figure 2; Box 1
1488				
1489	mitochondrial outer membrane	mtOM		MOM is widely used; the first M is replaced by mt; Figure 2; Box 1
1490				
1491	mitochondrial recovery	Y_{mtE}		fraction of mtE recovered in sample from the tissue of origin
1492				
1493	mitochondrial yield	$Y_{mtE/m}$		mt-yield per tissues mass; $Y_{mtE/m} = Y_{mtE} \cdot D_{mtE}$
1494				
1495	molar format	\underline{n}	$[\text{mol}]$	Table 6
1496	negative	neg		Figure 4
1497	number concentration of X	C_{NX}	$[\text{x} \cdot \text{m}^{-3}]$	Table 4
1498	number format	\underline{N}	$[\text{x}]$	Table 4; Figure 6
1499	number of cells	N_{ce}	$[\text{x}]$	$N_{ce} = N_{vce} + N_{dce}$; Table 5
1500	number of entities X	N_X	$[\text{x}]$	Table 4; Figure 6
1501	number of entity B	N_B	$[\text{x}]$	Table 4
1502	oxidative phosphorylation	OXPHOS		state; Table 1; Figure 4
1503	OXPHOS state	OXPHOS		Table 1; State 3 if $[\text{ADP}]$ and $[\text{P}_i]$ are saturating
1504				
1505	OXPHOS-capacity	P	<i>varies</i>	Table 1; Figure 4
1506	oxygen concentration	$c_{\text{O}_2} = n_{\text{O}_2} \cdot V^{-1}$	$[\text{mol} \cdot \text{m}^{-3}]$	$[\text{O}_2]$; Section 3.2
1507	oxygen flux, in reaction r	$J_{r\text{O}_2}$	<i>varies</i>	Figure 1
1508	pathway control state	PCS		Section 2.2
1509	permeability transition	mtPT		Figure 3; Section 2.4.3; MPT is widely used; M is replaced by mt
1510				
1511	permeabilized cell number	N_{pce}	$[\text{x}]$	experimental permeabilization of plasma membrane; Table 5
1512				
1513	phosphorylation of ADP to ATP	$P \gg$		Section 2.2
1514	$P \gg / \text{O}_2$ ratio	$P \gg / \text{O}_2$		mechanistic $Y_{P \gg / \text{O}_2}$, calculated from pump stoichiometries; Figure 2B
1515				
1516	positive	pos		Figure 4
1517	proton in the negative compartment	H^+_{neg}		Figure 4
1518	proton in the positive compartment	H^+_{pos}		Figure 4
1519	protonmotive force	pmf	$[\text{V}]$	Figures 1, 2A and 4; Table 1
1520	rate of electron transfer in ET state	E	<i>varies</i>	ET-capacity; Table 1
1521	rate of LEAK-respiration	L	<i>varies</i>	Table 1
1522	rate of oxidative phosphorylation	P	<i>varies</i>	OXPHOS-capacity; Table 1
1523	rate of residual oxygen consumption	ROx		Table 1; Figure 1
1524	residual oxygen consumption	ROX		state; Table 1
1525	respiratory supercomplex	SC I _n III _n IV _n		supramolecular assemblies composed of variable copy numbers (n) of CI, CIII and CIV; Box 1
1526				
1527				
1528	specific mitochondrial density	$D_{mtE} = mtE \cdot m_X^{-1}$	$[\text{mtEU} \cdot \text{kg}^{-1}]$	Table 4

1529	substrate-uncoupler-inhibitor-			
1530	titration protocol	SUIT		Section 2.2
1531	volume	V	$[m^{-3}]$	Table 7
1532	volume format	\underline{V}	$[m^{-3}]$	Table 6

1534
 1535 Experimentally, respiration is separated in mitochondrial preparations from the interactions with
 1536 the fermentative pathways of the intact cell. OXPHOS analysis is based on the study of mitochondrial
 1537 preparations complementary to bioenergetic investigations of (1) submitochondrial particles and
 1538 molecular structures, (2) intact cells, and (3) organisms—from model organisms to the human species
 1539 including healthy and diseased persons (patients). Different mechanisms of respiratory uncoupling have
 1540 to be distinguished (**Figure 3**). Metabolic fluxes measured in defined coupling and pathway control
 1541 states (**Figures 5 and 6**) provide insights into the meaning of cellular and organismic respiration.

1542 The optimal choice for expressing mitochondrial and cell respiration as O_2 flow per biological
 1543 sample, and normalization for specific tissue-markers (volume, mass, protein) and mitochondrial
 1544 markers (volume, protein, content, mtDNA, activity of marker enzymes, respiratory reference state) is
 1545 guided by the scientific question under study. Interpretation of the data depends critically on appropriate
 1546 normalization (**Figure 6**).

1547 MitoEAGLE can serve as a gateway to better diagnose mitochondrial respiratory adaptations and
 1548 defects linked to genetic variation, age-related health risks, sex-specific mitochondrial performance,
 1549 lifestyle with its effects on degenerative diseases, and thermal and chemical environment. The present
 1550 recommendations on coupling control states and rates, linked to the concept of the protonmotive force,
 1551 are focused on studies using mitochondrial preparations (**Box 3**). These will be extended in a series of
 1552 reports on pathway control of mitochondrial respiration, respiratory states in intact cells, and
 1553 harmonization of experimental procedures.

1554 **Acknowledgements**

1555 We thank Beno M for management assistance, and Rich PR for valuable discussions. This publication
 1556 is based upon work from COST Action CA15203 MitoEAGLE, supported by COST (European
 1557 Cooperation in Science and Technology), in cooperation with COST Actions CA16225 EU-
 1558 CARDIOPROTECTION and CA17129 CardioRNA, and K-Regio project MitoFit funded by the
 1559 Tyrolian Government.

1560 **Author contributions**

1561 This manuscript developed as an open invitation to scientists and students to join as coauthors in the
 1562 bottom-up spirit of COST, based on a first draft written by the corresponding author, who integrated
 1563 coauthor contributions in a sequence of Open Access versions. Coauthors contributed to the scope and
 1564 quality of the manuscript, may have focused on a particular section, and are listed in alphabetical order.
 1565 Coauthors confirm that they have read the final manuscript and agree to implement the
 1566 recommendations into future manuscripts, presentations and teaching materials.

1567 **Competing financial interests:** E.G. is founder and CEO of Oroboros Instruments, Innsbruck, Austria.

1570 **References**

- 1571
 1572
 1573
 1574 Altmann R (1894) Die Elementarorganismen und ihre Beziehungen zu den Zellen. Zweite vermehrte Auflage.
 1575 Verlag Von Veit & Comp, Leipzig:160 pp.
 1576 Baggeto LG, Testa-Perussini R (1990) Role of acetoin on the regulation of intermediate metabolism of Ehrlich
 1577 ascites tumor mitochondria: its contribution to membrane cholesterol enrichment modifying passive proton
 1578 permeability. Arch Biochem Biophys 283:341-8.
 1579 Beard DA (2005) A biophysical model of the mitochondrial respiratory system and oxidative phosphorylation.
 1580 PLoS Comput Biol 1(4):e36.
 1581 Benda C (1898) Weitere Mitteilungen über die Mitochondria. Verh Dtsch Physiol Ges:376-83.
 1582 Birkedal R, Laasmaa M, Vendelin M (2014) The location of energetic compartments affects energetic
 1583 communication in cardiomyocytes. Front Physiol 5:376.
 1584 Blier PU, Dufresne F, Burton RS (2001) Natural selection and the evolution of mtDNA-encoded peptides:
 1585 evidence for intergenomic co-adaptation. Trends Genet 17:400-6.

- 1586 Blier PU, Guderley HE (1993) Mitochondrial activity in rainbow trout red muscle: the effect of temperature on
1587 the ADP-dependence of ATP synthesis. *J Exp Biol* 176:145-58.
- 1588 Breton S, Beaupré HD, Stewart DT, Hoeh WR, Blier PU (2007) The unusual system of doubly uniparental
1589 inheritance of mtDNA: isn't one enough? *Trends Genet* 23:465-74.
- 1590 Brown GC (1992) Control of respiration and ATP synthesis in mammalian mitochondria and cells. *Biochem J*
1591 284:1-13.
- 1592 Burger G, Gray MW, Forget L, Lang BF (2013) Strikingly bacteria-like and gene-rich mitochondrial genomes
1593 throughout jakobid protists. *Genome Biol Evol* 5:418-38.
- 1594 Calvo SE, Klauser CR, Mootha VK (2016) MitoCarta2.0: an updated inventory of mammalian mitochondrial
1595 proteins. *Nucleic Acids Research* 44:D1251-7.
- 1596 Calvo SE, Julien O, Clauser KR, Shen H, Kamer KJ, Wells JA, Mootha VK (2017) Comparative analysis of
1597 mitochondrial N-termini from mouse, human, and yeast. *Mol Cell Proteomics* 16:512-23.
- 1598 Campos JC, Queliconi BB, Bozi LHM, Bechara LRG, Dourado PMM, Andres AM, Jannig PR, Gomes KMS,
1599 Zambelli VO, Rocha-Resende C, Guatimosim S, Brum PC, Mochly-Rosen D, Gottlieb RA, Kowaltowski AJ,
1600 Ferreira JCB (2017) Exercise reestablishes autophagic flux and mitochondrial quality control in heart failure.
1601 *Autophagy* 13:1304-317.
- 1602 Canton M, Luvisetto S, Schmehl I, Azzone GF (1995) The nature of mitochondrial respiration and discrimination
1603 between membrane and pump properties. *Biochem J* 310:477-81.
- 1604 Carrico C, Meyer JG, He W, Gibson BW, Verdin E (2018) The mitochondrial acylome emerges: proteomics,
1605 regulation by Sirtuins, and metabolic and disease implications. *Cell Metab* 27:497-512.
- 1606 Chan DC (2006) Mitochondria: dynamic organelles in disease, aging, and development. *Cell* 125:1241-52.
- 1607 Chance B, Williams GR (1955a) Respiratory enzymes in oxidative phosphorylation. I. Kinetics of oxygen
1608 utilization. *J Biol Chem* 217:383-93.
- 1609 Chance B, Williams GR (1955b) Respiratory enzymes in oxidative phosphorylation: III. The steady state. *J Biol*
1610 *Chem* 217:409-27.
- 1611 Chance B, Williams GR (1955c) Respiratory enzymes in oxidative phosphorylation. IV. The respiratory chain. *J*
1612 *Biol Chem* 217:429-38.
- 1613 Chance B, Williams GR (1956) The respiratory chain and oxidative phosphorylation. *Adv Enzymol Relat Subj*
1614 *Biochem* 17:65-134.
- 1615 Chowdhury SK, Djordjevic J, Albensi B, Fernyhough P (2015) Simultaneous evaluation of substrate-dependent
1616 oxygen consumption rates and mitochondrial membrane potential by TMRM and safranin in cortical
1617 mitochondria. *Biosci Rep* 36:e00286.
- 1618 Cobb LJ, Lee C, Xiao J, Yen K, Wong RG, Nakamura HK, Mehta HH, Gao Q, Ashur C, Huffman DM, Wan J,
1619 Muzumdar R, Barzilai N, Cohen P (2016) Naturally occurring mitochondrial-derived peptides are age-
1620 dependent regulators of apoptosis, insulin sensitivity, and inflammatory markers. *Aging (Albany NY)* 8:796-
1621 809.
- 1622 Cohen ER, Cvitas T, Frey JG, Holmström B, Kuchitsu K, Marquardt R, Mills I, Pavese F, Quack M, Stohner J,
1623 Strauss HL, Takami M, Thor HL (2008) Quantities, units and symbols in physical chemistry, IUPAC Green
1624 Book, 3rd Edition, 2nd Printing, IUPAC & RSC Publishing, Cambridge.
- 1625 Cooper H, Hedges LV, Valentine JC, eds (2009) The handbook of research synthesis and meta-analysis. Russell
1626 Sage Foundation.
- 1627 Coopersmith J (2010) Energy, the subtle concept. The discovery of Feynman's blocks from Leibnitz to Einstein.
1628 Oxford University Press:400 pp.
- 1629 Cummins J (1998) Mitochondrial DNA in mammalian reproduction. *Rev Reprod* 3:172-82.
- 1630 Dai Q, Shah AA, Garde RV, Yonish BA, Zhang L, Medvitz NA, Miller SE, Hansen EL, Dunn CN, Price TM
1631 (2013) A truncated progesterone receptor (PR-M) localizes to the mitochondrion and controls cellular
1632 respiration. *Mol Endocrinol* 27:741-53.
- 1633 Daum B, Walter A, Horst A, Osiewacz HD, Kühlbrandt W (2013) Age-dependent dissociation of ATP synthase
1634 dimers and loss of inner-membrane cristae in mitochondria. *Proc Natl Acad Sci U S A* 110:15301-6.
- 1635 Divakaruni AS, Brand MD (2011) The regulation and physiology of mitochondrial proton leak. *Physiology*
1636 (Bethesda) 26:192-205.
- 1637 Doerrier C, Garcia-Souza LF, Krumschnabel G, Wohlfarter Y, Mészáros AT, Gnaiger E (2018) High-Resolution
1638 Fluorescence Respirometry and OXPHOS protocols for human cells, permeabilized fibres from small biopsies of
1639 muscle, and isolated mitochondria. *Methods Mol Biol* 1782 (Palmeira CM, Moreno AJ, eds): Mitochondrial
1640 Bioenergetics, 978-1-4939-7830-4.
- 1641 Doskey CM, van 't Erve TJ, Wagner BA, Buettner GR (2015) Moles of a substance per cell is a highly informative
1642 dosing metric in cell culture. *PLoS One* 10:e0132572.
- 1643 Drahota Z, Milerová M, Stieglarová A, Houstek J, Ostádal B (2004) Developmental changes of cytochrome *c*
1644 oxidase and citrate synthase in rat heart homogenate. *Physiol Res* 53:119-22.
- 1645 Duarte FV, Palmeira CM, Rolo AP (2014) The role of microRNAs in mitochondria: small players acting wide.
1646 *Genes (Basel)* 5:865-86.

- 1647 Ehinger JK, Morota S, Hansson MJ, Paul G, Elmér E (2015) Mitochondrial dysfunction in blood cells from
 1648 amyotrophic lateral sclerosis patients. *J Neurol* 262:1493-503.
- 1649 Ernster L, Schatz G (1981) Mitochondria: a historical review. *J Cell Biol* 91:227s-55s.
- 1650 Estabrook RW (1967) Mitochondrial respiratory control and the polarographic measurement of ADP:O ratios.
 1651 *Methods Enzymol* 10:41-7.
- 1652 Faber C, Zhu ZJ, Castellino S, Wagner DS, Brown RH, Peterson RA, Gates L, Barton J, Bickett M, Hagerty L,
 1653 Kimbrough C, Sola M, Bailey D, Jordan H, Elangbam CS (2014) Cardiolipin profiles as a potential biomarker
 1654 of mitochondrial health in diet-induced obese mice subjected to exercise, diet-restriction and ephedrine
 1655 treatment. *J Appl Toxicol* 34:1122-9.
- 1656 Feagin JE, Harrell MI, Lee JC, Coe KJ, Sands BH, Cannone JJ, Tami G, Schnare MN, Gutell RR (2012) The
 1657 fragmented mitochondrial ribosomal RNAs of *Plasmodium falciparum*. *PLoS One* 7:e38320.
- 1658 Fell D (1997) Understanding the control of metabolism. Portland Press.
- 1659 Forstner H, Gnaiger E (1983) Calculation of equilibrium oxygen concentration. In: Polarographic Oxygen Sensors.
 1660 Aquatic and Physiological Applications. Gnaiger E, Forstner H (eds), Springer, Berlin, Heidelberg, New
 1661 York:321-33.
- 1662 Garlid KD, Beavis AD, Ratkje SK (1989) On the nature of ion leaks in energy-transducing membranes. *Biochim*
 1663 *Biophys Acta* 976:109-20.
- 1664 Garlid KD, Semrad C, Zinchenko V. Does redox slip contribute significantly to mitochondrial respiration? In:
 1665 Schuster S, Rigoulet M, Ouhabi R, Mazat J-P, eds (1993) Modern trends in biothermokinetics. Plenum Press,
 1666 New York, London:287-93.
- 1667 Gerö D, Szabo C (2016) Glucocorticoids suppress mitochondrial oxidant production via upregulation of
 1668 uncoupling protein 2 in hyperglycemic endothelial cells. *PLoS One* 11:e0154813.
- 1669 Gnaiger E. Efficiency and power strategies under hypoxia. Is low efficiency at high glycolytic ATP production a
 1670 paradox? In: Surviving Hypoxia: Mechanisms of Control and Adaptation. Hochachka PW, Lutz PL, Sick T,
 1671 Rosenthal M, Van den Thillart G, eds (1993a) CRC Press, Boca Raton, Ann Arbor, London, Tokyo:77-109.
- 1672 Gnaiger E (1993b) Nonequilibrium thermodynamics of energy transformations. *Pure Appl Chem* 65:1983-2002.
- 1673 Gnaiger E (2001) Bioenergetics at low oxygen: dependence of respiration and phosphorylation on oxygen and
 1674 adenosine diphosphate supply. *Respir Physiol* 128:277-97.
- 1675 Gnaiger E (2009) Capacity of oxidative phosphorylation in human skeletal muscle. New perspectives of
 1676 mitochondrial physiology. *Int J Biochem Cell Biol* 41:1837-45.
- 1677 Gnaiger E (2014) Mitochondrial pathways and respiratory control. An introduction to OXPHOS analysis. 4th ed.
 1678 *Mitochondr Physiol Network* 19.12. Oroboros MiPNet Publications, Innsbruck:80 pp.
- 1679 Gnaiger E, Méndez G, Hand SC (2000) High phosphorylation efficiency and depression of uncoupled respiration
 1680 in mitochondria under hypoxia. *Proc Natl Acad Sci USA* 97:11080-5.
- 1681 Greggio C, Jha P, Kulkarni SS, Lagarrigue S, Broskey NT, Boutant M, Wang X, Conde Alonso S, Ofori E, Auwerx
 1682 J, Cantó C, Amati F (2017) Enhanced respiratory chain supercomplex formation in response to exercise in
 1683 human skeletal muscle. *Cell Metab* 25:301-11.
- 1684 Hinkle PC (2005) P/O ratios of mitochondrial oxidative phosphorylation. *Biochim Biophys Acta* 1706:1-11.
- 1685 Hofstadter DR (1979) Gödel, Escher, Bach: An eternal golden braid. A metaphorical fugue on minds and machines
 1686 in the spirit of Lewis Carroll. Harvester Press:499 pp.
- 1687 Illaste A, Laasmaa M, Peterson P, Vendelin M (2012) Analysis of molecular movement reveals latticelike
 1688 obstructions to diffusion in heart muscle cells. *Biophys J* 102:739-48.
- 1689 Jasienski M, Bazzaz FA (1999) The fallacy of ratios and the testability of models in biology. *Oikos* 84:321-26.
- 1690 Jepihhina N, Beraud N, Sepp M, Birkedal R, Vendelin M (2011) Permeabilized rat cardiomyocyte response
 1691 demonstrates intracellular origin of diffusion obstacles. *Biophys J* 101:2112-21.
- 1692 Jezek P, Holendova B, Garlid KD, Jaburek M (2018) Mitochondrial uncoupling proteins: subtle regulators of
 1693 cellular redox signaling. *Antioxid Redox Signal* 29:667-714.
- 1694 Karnkowska A, Vacek V, Zubáčová Z, Treitli SC, Petrželková R, Eme L, Novák L, Žárský V, Barlow LD, Herman
 1695 EK, Soukal P, Hroudová M, Doležal P, Stairs CW, Roger AJ, Eliáš M, Dacks JB, Vlček Č, Hampl V (2016) A
 1696 eukaryote without a mitochondrial organelle. *Curr Biol* 26:1274-84.
- 1697 Kenwood BM, Weaver JL, Bajwa A, Poon IK, Byrne FL, Murrow BA, Calderone JA, Huang L, Divakaruni AS,
 1698 Tomsig JL, Okabe K, Lo RH, Cameron Coleman G, Columbus L, Yan Z, Saucerman JJ, Smith JS, Holmes
 1699 JW, Lynch KR, Ravichandran KS, Uchiyama S, Santos WL, Rogers GW, Okusa MD, Bayliss DA, Hoehn KL
 1700 (2013) Identification of a novel mitochondrial uncoupler that does not depolarize the plasma membrane. *Mol*
 1701 *Metab* 3:114-23.
- 1702 Klepinin A, Ounpuu L, Guzun R, Chekulayev V, Timohhina N, Tepp K, Shevchuk I, Schlattner U, Kaambre T
 1703 (2016) Simple oxygraphic analysis for the presence of adenylate kinase 1 and 2 in normal and tumor cells. *J*
 1704 *Bioenerg Biomembr* 48:531-48.
- 1705 Koit A, Shevchuk I, Ounpuu L, Klepinin A, Chekulayev V, Timohhina N, Tepp K, Puurand M, Truu L, Heck K,
 1706 Valvere V, Guzun R, Kaambre T (2017) Mitochondrial respiration in human colorectal and breast cancer
 1707 clinical material is regulated differently. *Oxid Med Cell Longev* 1372640.

- 1708 Komlódi T, Tretter L (2017) Methylene blue stimulates substrate-level phosphorylation catalysed by succinyl-
 1709 CoA ligase in the citric acid cycle. *Neuropharmacology* 123:287-98.
- 1710 Korn E (1969) Cell membranes: structure and synthesis. *Annu Rev Biochem* 38:263–88.
- 1711 Lai N, M Kummitha C, Rosca MG, Fujioka H, Tandler B, Hoppel CL (2018) Isolation of mitochondrial
 1712 subpopulations from skeletal muscle: optimizing recovery and preserving integrity. *Acta Physiol*
 1713 (Oxf):e13182. doi: 10.1111/apha.13182.
- 1714 Lane N (2005) Power, sex, suicide: mitochondria and the meaning of life. Oxford University Press:354 pp.
- 1715 Larsen S, Nielsen J, Neigaard Nielsen C, Nielsen LB, Wibrand F, Stride N, Schroder HD, Boushel RC, Helge JW,
 1716 Dela F, Hey-Mogensen M (2012) Biomarkers of mitochondrial content in skeletal muscle of healthy young
 1717 human subjects. *J Physiol* 590:3349-60.
- 1718 Lee C, Zeng J, Drew BG, Sallam T, Martin-Montalvo A, Wan J, Kim SJ, Mehta H, Hevener AL, de Cabo R,
 1719 Cohen P (2015) The mitochondrial-derived peptide MOTS-c promotes metabolic homeostasis and reduces
 1720 obesity and insulin resistance. *Cell Metab* 21:443-54.
- 1721 Lee SR, Kim HK, Song IS, Youm J, Dizon LA, Jeong SH, Ko TH, Heo HJ, Ko KS, Rhee BD, Kim N, Han J
 1722 (2013) Glucocorticoids and their receptors: insights into specific roles in mitochondria. *Prog Biophys Mol Biol*
 1723 112:44-54.
- 1724 Leek BT, Mudaliar SR, Henry R, Mathieu-Costello O, Richardson RS (2001) Effect of acute exercise on citrate
 1725 synthase activity in untrained and trained human skeletal muscle. *Am J Physiol Regul Integr Comp Physiol*
 1726 280:R441-7.
- 1727 Lemasters JJ, Nieminen AL, Qian T, Trost LC, Elmore SP, Nishimura Y, Crowe RA, Cascio WE, Bradham CA,
 1728 Brenner DA, Herman B (1998) The mitochondrial permeability transition in cell death: a common mechanism
 1729 in necrosis, apoptosis and autophagy. *Biochim Biophys Acta* 1366:177-96.
- 1730 Lemieux H, Blier PU, Gnaiger E (2017) Remodeling pathway control of mitochondrial respiratory capacity by
 1731 temperature in mouse heart: electron flow through the Q-junction in permeabilized fibers. *Sci Rep* 7:2840.
- 1732 Lenaz G, Tioli G, Falasca AI, Genova ML (2017) Respiratory supercomplexes in mitochondria. In: *Mechanisms*
 1733 *of primary energy trasduction in biology*. M Wikstrom (ed) Royal Society of Chemistry Publishing, London,
 1734 UK:296-337.
- 1735 Liu S, Roellig DM, Guo Y, Li N, Frace MA, Tang K, Zhang L, Feng Y, Xiao L (2016) Evolution of mitosome
 1736 metabolism and invasion-related proteins in *Cryptosporidium*. *BMC Genomics* 17:1006.
- 1737 Luo S, Valencia CA, Zhang J, Lee NC, Slone J, Gui B, Wang X, Li Z, Dell S, Brown J, Chen SM, Chien YH,
 1738 Hwu WL, Fan PC, Wong LJ, Atwal PS, Huang T (2018) Biparental inheritance of mitochondrial DNA in
 1739 humans. *Proc Natl Acad Sci U S A* doi: 10.1073/pnas.1810946115.
- 1740 Margulis L (1970) Origin of eukaryotic cells. New Haven: Yale University Press.
- 1741 McDonald AE, Vanlerberghe GC, Staples JF (2009) Alternative oxidase in animals: unique characteristics and
 1742 taxonomic distribution. *J Exp Biol* 212:2627-34.
- 1743 Menshikova EV, Ritov VB, Fairfull L, Ferrell RE, Kelley DE, Goodpaster BH (2006) Effects of exercise on
 1744 mitochondrial content and function in aging human skeletal muscle. *J Gerontol A Biol Sci Med Sci* 61:534-40.
- 1745 Menshikova EV, Ritov VB, Ferrell RE, Azuma K, Goodpaster BH, Kelley DE (2007) Characteristics of skeletal
 1746 muscle mitochondrial biogenesis induced by moderate-intensity exercise and weight loss in obesity. *J Appl*
 1747 *Physiol* (1985) 103:21-7.
- 1748 Menshikova EV, Ritov VB, Toledo FG, Ferrell RE, Goodpaster BH, Kelley DE (2005) Effects of weight loss and
 1749 physical activity on skeletal muscle mitochondrial function in obesity. *Am J Physiol Endocrinol Metab*
 1750 288:E818-25.
- 1751 Miller GA (1991) The science of words. Scientific American Library New York:276 pp.
- 1752 Mitchell P (1961) Coupling of phosphorylation to electron and hydrogen transfer by a chemi-osmotic type of
 1753 mechanism. *Nature* 191:144-8.
- 1754 Mitchell P (2011) Chemiosmotic coupling in oxidative and photosynthetic phosphorylation. *Biochim Biophys*
 1755 *Acta Bioenergetics* 1807:1507-38.
- 1756 Mogensen M, Sahlin K, Fernström M, Glintborg D, Vind BF, Beck-Nielsen H, Højlund K (2007) Mitochondrial
 1757 respiration is decreased in skeletal muscle of patients with type 2 diabetes. *Diabetes* 56:1592-9.
- 1758 Mohr PJ, Phillips WD (2015) Dimensionless units in the SI. *Metrologia* 52:40-7.
- 1759 Moreno M, Giacco A, Di Munno C, Goglia F (2017) Direct and rapid effects of 3,5-diiodo-L-thyronine (T2). *Mol*
 1760 *Cell Endocrinol* 7207:30092-8.
- 1761 Morrow RM, Picard M, Derbeneva O, Leipzig J, McManus MJ, Gouspillou G, Barbat-Artigas S, Dos Santos C,
 1762 Hepple RT, Murdock DG, Wallace DC (2017) Mitochondrial energy deficiency leads to hyperproliferation of
 1763 skeletal muscle mitochondria and enhanced insulin sensitivity. *Proc Natl Acad Sci U S A* 114:2705-10.
- 1764 Murley A, Nunnari J (2016) The emerging network of mitochondria-organelle contacts. *Mol Cell* 61:648-53.
- 1765 National Academies of Sciences, Engineering, and Medicine (2018) International coordination for science data
 1766 infrastructure: Proceedings of a workshop—in brief. Washington, DC: The National Academies Press. doi:
 1767 <https://doi.org/10.17226/25015>.

- 1768 Oemer G, Lackner L, Muigg K, Krumschnabel G, Watschinger K, Sailer S, Lindner H, Gnaiger E, Wortmann SB,
 1769 Werner ER, Zschocke J, Keller MA (2018) The molecular structural diversity of mitochondrial cardiolipins.
 1770 Proc Nat Acad Sci U S A 115:4158-63.
- 1771 Palmfeldt J, Bross P (2017) Proteomics of human mitochondria. Mitochondrion 33:2-14.
- 1772 Paradies G, Paradies V, De Benedictis V, Ruggiero FM, Petrosillo G (2014) Functional role of cardiolipin in
 1773 mitochondrial bioenergetics. Biochim Biophys Acta 1837:408-17.
- 1774 Pesta D, Gnaiger E (2012) High-Resolution Respirometry. OXPHOS protocols for human cells and permeabilized
 1775 fibres from small biopsies of human muscle. Methods Mol Biol 810:25-58.
- 1776 Pesta D, Hoppel F, Macek C, Messner H, Faulhaber M, Kobel C, Parson W, Burtscher M, Schocke M, Gnaiger E
 1777 (2011) Similar qualitative and quantitative changes of mitochondrial respiration following strength and
 1778 endurance training in normoxia and hypoxia in sedentary humans. Am J Physiol Regul Integr Comp Physiol
 1779 301:R1078-87.
- 1780 Price TM, Dai Q (2015) The role of a mitochondrial progesterone receptor (PR-M) in progesterone action. Semin
 1781 Reprod Med 33:185-94.
- 1782 Puchowicz MA, Varnes ME, Cohen BH, Friedman NR, Kerr DS, Hoppel CL (2004) Oxidative phosphorylation
 1783 analysis: assessing the integrated functional activity of human skeletal muscle mitochondria – case studies.
 1784 Mitochondrion 4:377-85. Puntschart A, Claassen H, Jostarndt K, Hoppeler H, Billetter R (1995) mRNAs of
 1785 enzymes involved in energy metabolism and mtDNA are increased in endurance-trained athletes. Am J Physiol
 1786 269:C619-25.
- 1787 Quiros PM, Mottis A, Auwerx J (2016) Mitonuclear communication in homeostasis and stress. Nat Rev Mol Cell
 1788 Biol 17:213-26.
- 1789 Rackham O, Mercer TR, Filipovska A (2012) The human mitochondrial transcriptome and the RNA-binding
 1790 proteins that regulate its expression. WIREs RNA 3:675-95.
- 1791 Rackham O, Shearwood AM, Mercer TR, Davies SM, Mattick JS, Filipovska A (2011) Long noncoding RNAs
 1792 are generated from the mitochondrial genome and regulated by nuclear-encoded proteins. RNA 17:2085-93.
- 1793 Reichmann H, Hoppeler H, Mathieu-Costello O, von Bergen F, Pette D (1985) Biochemical and ultrastructural
 1794 changes of skeletal muscle mitochondria after chronic electrical stimulation in rabbits. Pflugers Arch 404:1-9.
- 1795 Renner K, Amberger A, Konwalinka G, Gnaiger E (2003) Changes of mitochondrial respiration, mitochondrial
 1796 content and cell size after induction of apoptosis in leukemia cells. Biochim Biophys Acta 1642:115-23.
- 1797 Rice DW, Alverson AJ, Richardson AO, Young GJ, Sanchez-Puerta MV, Munzinger J, Barry K, Boore JL, Zhang
 1798 Y, dePamphilis CW, Knox EB, Palmer JD (2016) Horizontal transfer of entire genomes via mitochondrial
 1799 fusion in the angiosperm *Amborella*. Science 342:1468-73.
- 1800 Rich P (2003) Chemiosmotic coupling: The cost of living. Nature 421:583.
- 1801 Rich PR (2013) Chemiosmotic theory. Encyclopedia Biol Chem 1:467-72.
- 1802 Roger JA, Munoz-Gomes SA, Kamikawa R (2017) The origin and diversification of mitochondria. Curr Biol
 1803 27:R1177-92.
- 1804 Rostovtseva TK, Sheldon KL, Hassanzadeh E, Monge C, Saks V, Bezrukov SM, Sackett DL (2008) Tubulin
 1805 binding blocks mitochondrial voltage-dependent anion channel and regulates respiration. Proc Natl Acad Sci
 1806 USA 105:18746-51.
- 1807 Rustin P, Parfait B, Chretien D, Bourgeron T, Djouadi F, Bastin J, Rötig A, Munnich A (1996) Fluxes of
 1808 nicotinamide adenine dinucleotides through mitochondrial membranes in human cultured cells. J Biol Chem
 1809 271:14785-90.
- 1810 Saks VA, Veksler VI, Kuznetsov AV, Kay L, Sikk P, Tiivel T, Tranqui L, Olivares J, Winkler K, Wiedemann F,
 1811 Kunz WS (1998) Permeabilised cell and skinned fiber techniques in studies of mitochondrial function in vivo.
 1812 Mol Cell Biochem 184:81-100.
- 1813 Salabei JK, Gibb AA, Hill BG (2014) Comprehensive measurement of respiratory activity in permeabilized cells
 1814 using extracellular flux analysis. Nat Protoc 9:421-38.
- 1815 Sazanov LA (2015) A giant molecular proton pump: structure and mechanism of respiratory complex I. Nat Rev
 1816 Mol Cell Biol 16:375-88.
- 1817 Schneider TD (2006) Claude Shannon: biologist. The founder of information theory used biology to formulate the
 1818 channel capacity. IEEE Eng Med Biol Mag 25:30-3.
- 1819 Schönfeld P, Dymkowska D, Wojtczak L (2009) Acyl-CoA-induced generation of reactive oxygen species in
 1820 mitochondrial preparations is due to the presence of peroxisomes. Free Radic Biol Med 47:503-9.
- 1821 Schultz J, Wiesner RJ (2000) Proliferation of mitochondria in chronically stimulated rabbit skeletal muscle--
 1822 transcription of mitochondrial genes and copy number of mitochondrial DNA. J Bioenerg Biomembr 32:627-
 1823 34.
- 1824 Speijer D (2016) Being right on Q: shaping eukaryotic evolution. Biochem J 473:4103-27.
- 1825 Sugiura A, Mattie S, Prudent J, McBride HM (2017) Newly born peroxisomes are a hybrid of mitochondrial and
 1826 ER-derived pre-peroxisomes. Nature 542:251-4.
- 1827 Simson P, Jephthina N, Laasmaa M, Peterson P, Birkedal R, Vendelin M (2016) Restricted ADP movement in
 1828 cardiomyocytes: Cytosolic diffusion obstacles are complemented with a small number of open mitochondrial
 1829 voltage-dependent anion channels. J Mol Cell Cardiol 97:197-203.

- 1830 Singh BK, Sinha RA, Tripathi M, Mendoza A, Ohba K, Sy JAC, Xie SY, Zhou J, Ho JP, Chang CY, Wu Y,
 1831 Giguère V, Bay BH, Vanacker JM, Ghosh S, Gauthier K, Hollenberg AN, McDonnell DP, Yen PM (2018)
 1832 Thyroid hormone receptor and ERR α coordinately regulate mitochondrial fission, mitophagy, biogenesis, and
 1833 function. *Sci Signal* 11(536) DOI: 10.1126/scisignal.aam5855.
- 1834 Stucki JW, Ineichen EA (1974) Energy dissipation by calcium recycling and the efficiency of calcium transport in
 1835 rat-liver mitochondria. *Eur J Biochem* 48:365-75.
- 1836 Tonkonogi M, Harris B, Sahlin K (1997) Increased activity of citrate synthase in human skeletal muscle after a
 1837 single bout of prolonged exercise. *Acta Physiol Scand* 161:435-6.
- 1838 Torralba D, Baixauli F, Sánchez-Madrid F (2016) Mitochondria know no boundaries: mechanisms and functions
 1839 of intercellular mitochondrial transfer. *Front Cell Dev Biol* 4:107. eCollection 2016.
- 1840 Vamecq J, Schepers L, Parmentier G, Mannaerts GP (1987) Inhibition of peroxisomal fatty acyl-CoA oxidase by
 1841 antimycin A. *Biochem J* 248:603-7.
- 1842 Waczulikova I, Habodaszova D, Cagalinec M, Ferko M, Ulicna O, Mateasik A, Sikurova L, Ziegelhöffer A (2007)
 1843 Mitochondrial membrane fluidity, potential, and calcium transients in the myocardium from acute diabetic rats.
 1844 *Can J Physiol Pharmacol* 85:372-81.
- 1845 Wagner BA, Venkataraman S, Buettner GR (2011) The rate of oxygen utilization by cells. *Free Radic Biol Med*
 1846 51:700-712.
- 1847 Wang H, Hiatt WR, Barstow TJ, Brass EP (1999) Relationships between muscle mitochondrial DNA content,
 1848 mitochondrial enzyme activity and oxidative capacity in man: alterations with disease. *Eur J Appl Physiol*
 1849 *Occup Physiol* 80:22-7.
- 1850 Watt IN, Montgomery MG, Runswick MJ, Leslie AG, Walker JE (2010) Bioenergetic cost of making an adenosine
 1851 triphosphate molecule in animal mitochondria. *Proc Natl Acad Sci U S A* 107:16823-7.
- 1852 Weibel ER, Hoppeler H (2005) Exercise-induced maximal metabolic rate scales with muscle aerobic capacity. *J*
 1853 *Exp Biol* 208:1635–44.
- 1854 White DJ, Wolff JN, Pierson M, Gemmell NJ (2008) Revealing the hidden complexities of mtDNA inheritance.
 1855 *Mol Ecol* 17:4925–42.
- 1856 Wikström M, Hummer G (2012) Stoichiometry of proton translocation by respiratory complex I and its
 1857 mechanistic implications. *Proc Natl Acad Sci U S A* 109:4431-6.
- 1858 Williams EG, Wu Y, Jha P, Dubuis S, Blattmann P, Argmann CA, Houten SM, Amariuta T, Wolski W, Zamboni
 1859 N, Aebersold R, Auwerx J (2016) Systems proteomics of liver mitochondria function. *Science* 352
 1860 (6291):aad0189
- 1861 Willis WT, Jackman MR, Messer JI, Kuzmiak-Glancy S, Glancy B (2016) A simple hydraulic analog model of
 1862 oxidative phosphorylation. *Med Sci Sports Exerc* 48:990-1000.
- 1863 Zíková A, Hampl V, Paris Z, Týč J, Lukeš J (2016) Aerobic mitochondria of parasitic protists: diverse genomes
 1864 and complex functions. *Mol Biochem Parasitol* 209:46-57.

1866 Supplement

1868 S1. Manuscript phases and versions - an open-access approach

1870 This manuscript on ‘Mitochondrial respiratory states and rates’ is a position statement in the frame of COST Action
 1871 CA15203 MitoEAGLE. The global MitoEAGLE network made it possible to collaborate with a large number of
 1872 coauthors to reach consensus on the present manuscript. Nevertheless, we do not consider scientific progress to be
 1873 supported by ‘declaration’ statements (other than on ethical or political issues). Our manuscript aims at providing
 1874 arguments for further debate rather than pushing opinions. We hope to initiate a much broader process of
 1875 discussion and want to raise the awareness of the importance of a consistent terminology for reporting of scientific
 1876 data in the field of bioenergetics, mitochondrial physiology and pathology. Quality of research requires quality of
 1877 communication. Some established researchers in the field may not want to re-consider the use of jargon which has
 1878 become established despite deficiencies of accuracy and meaning. In the long run, superior standards will become
 1879 accepted. We hope to contribute to this evolutionary process, with an emphasis on harmonization rather than
 1880 standardization.

1881 *Phase 1* The protonmotive force and respiratory control

1882 http://www.mitoeagle.org/index.php/The_protonmotive_force_and_respiratory_control

- 1883 • 2017-04-09 to 2017-09-18 (44 versions) / 2017-09-21 to 2018-02-06 (44 plus 21 versions)

1884 http://www.mitoeagle.org/index.php/MitoEAGLE_preprint_2017-09-21

1885 2017-11-11: Print version (16) for MiP2017/MitoEAGLE conference in Hradec Kralove

1886 *Phase 2* Mitochondrial respiratory states and rates: Building blocks of mitochondrial physiology Part 1

1887 http://www.mitoeagle.org/index.php/MitoEAGLE_preprint_States_and_rates

- 1888 • 2018-02-08 – 2018-12-12 (44 plus 50 Versions)


1889 *Phase 3* 2018-12-12: Mitochondrial respiratory states and rates. Submission to a preprint server

1890 *Phase 4* Journal submission: CELL METABOLISM, aiming at indexing by *The Web of Science* and *PubMed*.

1891
1892
1893
1894
1895
1896

S2. Joining COST Actions

- CA15203 MitoEAGLE - http://www.cost.eu/COST_Actions/ca/CA15203
- CA16225 EU-CARDIOPROTECTION - http://www.cost.eu/COST_Actions/ca/CA16225
- CA17129 CardioRNA - http://www.cost.eu/COST_Actions/ca/CA17129



Mitochondrial respiratory states and rates:

Building blocks of mitochondrial physiology

Part 1 - www.mitoeagle.org/index.php/MitoEAGLE_preprint_2018-02-08

Gnaiger E^{1,2}, corresponding author
355 co-authors, MitoEAGLE Working Group

¹Medical University Innsbruck
²Oroboros, Innsbruck, Austria

Aims

Clarity of concept and consistency of nomenclature facilitate effective transdisciplinary communication, education, and ultimately further discovery.

Adhering to uniform standards and harmonizing the terminology concerning mitochondrial respiratory states and rates will support the development of databases of mitochondrial respiratory function in cells, tissues, and species.

Summary

Recommendations on coupling control states and rates are focused on studies with mitochondrial preparations.

Fig. 1: Respiration is defined by O₂ flux balance.

Fig. 2: OXPHOS analysis is based on the study of mt- preparations. Metabolic fluxes measured in defined coupling and pathway control states provide insights into the meaning of cellular respiration.

Fig. 3: Interpretation of respiratory rates depends critically on appropriate normalization.

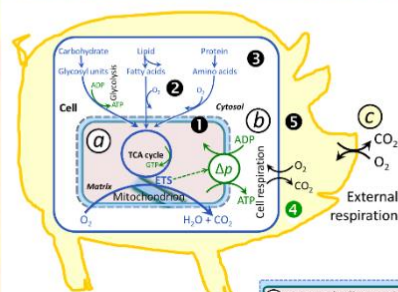


Figure 2. Respiratory states (ET, OXPHOS, LEAK) and corresponding rates (E, P, L)

Net OXPHOS-capacity, P-L, and excess capacity, E-P.

State	J _{ko}	J _p	Δp	Inducing factors	Limiting factors
LEAK	L; low, cation leak-dependent respiration	0	max.	proton leak, slip, and cation cycling	J _p = 0: (1) without ADP, L _S ; (2) max. ATP/ADP ratio, L _T ; or (3) inhibition of the phosphorylation-pathway, L _{Only}
OXPHOS	P; high, ADP-stimulated respiration	max.	high	kinetically-saturating [ADP] and [P _i]	J _p by phosphorylation-pathway, or J _{ko} by ET-capacity
ET	E; max., noncoupled respiration	0	low	optimal external uncoupler concentration for max. J _{oL,E}	J _{ko} by ET-capacity
ROX	Rox; min., residual O ₂ consumption	0	0	J _{oL,Rox} in non-ET-pathway oxidation reactions	inhibition of all ET-pathways; or absence of fuel substrates

Figure 1. From mitochondrial to external respiration

Mitochondrial (mt) respiration is the oxidation of fuel substrates (electron donors) and reduction of O₂ catalysed by the electron transfer system, ETS:

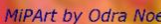
- (a) mt-catabolic respiration, excluding
- (b) mt-residual oxygen consumption, R_{ox}.
- (c) Total cellular O₂ consumption, including mt-R_{ox}, (d) non-mt catabolic R_{ox}, particularly by peroxisomal oxidases, and (e) non-mt R_{ox} unrelated to catabolism.


External respiration, including aerobic microbial respiration, and extracellular O₂ consumption.

Figure 3. Normalization of rate

A: Cell respiration is normalized for (1) the experimental Sample (flow per object, mass-specific flux, or cell-volume-specific flux); or (2) for methodological reasons for the Chamber volume.

B: Flow per cell [amol O₂ s⁻¹·cell⁻¹] is flux per chamber volume, J_V [nmol O₂·s⁻¹·L⁻¹], divided by cell concentration in the chamber, N_{cell}/V [cells·L⁻¹], which is Number analysis. In Structure analysis, aerobic cell performance is mt-quality (mt-specific flux, e.g., per citrate synthase, CS) times mt-quantity, or mt-function times mt-structure.





Funded by the Horizon 2020 Framework Programme of the European Union

MitoEAGLE
Join
COST Action CA15203
www.mitoeagle.org/index.php/MitoEAGLE

**COST Action
CA15203**

MitoEAGLE

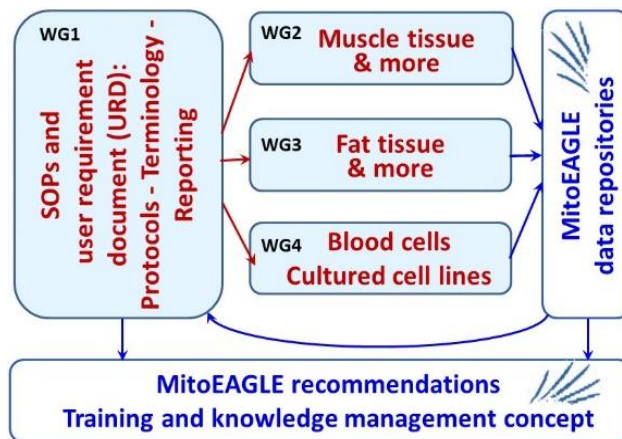
**Evolution Age Gender
Lifestyle Environment**



Mission of the global MitoEAGLE network

in collaboration with the Mitochondrial Physiology Society, MiPs

- Improve our knowledge on mitochondrial function in health and disease with regard to Evolution, Age, Gender, Lifestyle and Environment
- Interrelate studies across laboratories with the help of a MitoEAGLE data management system
- Provide standardized measures to link mitochondrial and physiological performance to understand the myriad of factors that play a role in mitochondrial physiology



Join the COST Action MitoEAGLE - contribute to the quality management network.



More information:
www.mitoeagle.org



Funded by the Horizon 2020 Framework Programme of the European Union

